Hydrodynamics of bacterial colonies: A model

J. Lega[1,*] and T. Passot[2,†]
[1]*Department of Mathematics, University of Arizona, 617 North Santa Rita, Tucson, Arizona 85721*
[2]*CNRS, Observatoire de la Côte d'Azur, Boîte Postale 4229, 06304 Nice Cedex 4, France*
(Received 26 October 2002; published 13 March 2003)

We propose a hydrodynamic model for the evolution of bacterial colonies growing on soft agar plates. This model consists of reaction-diffusion equations for the concentrations of nutrients, water, and bacteria, coupled to a single hydrodynamic equation for the velocity field of the bacteria-water mixture. It captures the dynamics inside the colony as well as on its boundary and allows us to identify a mechanism for collective motion towards fresh nutrients, which, in its modeling aspects, is similar to classical chemotaxis. As shown in numerical simulations, our model reproduces both usual colony shapes and typical hydrodynamic motions, such as the whirls and jets recently observed in wet colonies of *Bacillus subtilis*. The approach presented here could be extended to different experimental situations and provides a general framework for the use of advection-reaction-diffusion equations in modeling bacterial colonies.

DOI: 10.1103/PhysRevE.67.031906 PACS number(s): 87.10.+e, 07.05.Tp, 87.18.Ed, 87.18.Bb

I. INTRODUCTION

The growth of bacterial colonies in the form of films or chains is an example of simple multicellular organization found in nature [1]. Remarkably rich behaviors have been observed in colonies of bacteria forced to develop on top of a gel (agar) containing nutrients. Expansion and growth of the colony is observed, during which cells translocate towards regions of fresh nutrients. Depending on the wetness of the growth medium and on the nutrient concentration, the colony boundary may take fascinating shapes, which are sometimes reminiscent of fractal structures [2–6]. The phase diagrams established in Refs. [4,6–10], which classify the shape of the colony in terms of wetness and nutrient concentration, show that the morphology of the colony is extremely sensitive to these two parameters. Patterns in the form of terraces, rings, and spots have also been observed inside bacterial colonies [11–14]. The nature of these spatial structures depends on the growth medium and on the type of bacteria used, which often secrete some chemoattractant. As stated in Ref. [15], understanding the shape and dynamics of laboratory grown colonies has significant impact ''in many realms of science, ranging from acquiring a deeper knowledge of prokaryotic cell biology to answering fundamental questions of genetics, evolution and morphogenesis.''

Colony expansion is phenomenologically modeled in terms of reaction-diffusion equations for nutrients and cell density. These equations may involve cell multiplication and death, linear or nonlinear diffusion, and chemotactic response to nutrients or to other chemicals secreted by the bacteria [6,16–19]. Such models typically reproduce the motion of a front corresponding to the boundary of the expanding colony. Depending on the model and on its parameters, this front may become unstable and lead to the formation of branched structures [6,19]. By taking into account the presence of motile and nonmotile bacteria as well as the existence of respiratory waste products and chemoattractants emitted by the bacteria, the formation of concentric rings and spots within the colony is also accounted for [20–22]. This approach can be generalized to other types of bacterial translocation, as discussed in Ref. [23] for swarmer cells. At a more microscopic level, fractal-like colony boundaries can be reproduced by a ''communicating walkers'' model, in which ensembles of bacteria at a mesoscopic scale constitute random walkers which receive energy by consuming nutrients and use energy at a constant rate [24]. In such a model, which also captures the response of the colony to anisotropy [25], the boundary of the colony moves when it has been hit by enough walkers in the course of their random walk.

Recent experiments described in Ref. [26] have shown that, in wet conditions, strains of *Bacillus subtilis* growing on an agar plate may form eddies and jets of bacteria (see also Ref. [4]). Such structures appear in the wetter regions of the colony and have a size that is intermediate between that of a single bacterium and that of the entire colony. In these experiments, the growth medium is very wet, so that bacteria swim and do not swarm, and nutrients are plentiful, at least initially. Moreover, the bacteria used in Ref. [26] do not produce surfactant [9]. As a consequence, the growth rate of the colony size is much smaller than for surfactant-producing strains, as exemplified in the experiments of Mendelson and Salhi [9]. Three levels of organization are observed in the colony: individual cell motion at a microscopic scale, whirls and jets at a mesoscopic scale, and a macroscopic superpattern of counter-rotating whirls. Some of the conclusions of Ref. [26] are that whirls and jets are ''produced by swimming in high cell density populations, not by classical swarming,'' that the motion of the colony boundary is influenced by whirls and jets, and that ''understanding the control of these complex events and their relationship to known aspects of bacterial swimming and taxis presents a new challenge to both microbiologists and physicists.'' More recently, intermittent whirls and jets formed by bacteria were also observed in a quasi-two-dimensional bath of *Escherichia coli* [27]. Even though it is not clear whether both experiments were performed in the same range of bacterial density, the

*Electronic address: lega@math.arizona.edu
†Electronic address: passot@obs-nice.fr

spontaneous formation of coherent structures in bacterial colonies confined to an almost two-dimensional domain appears to be quite general [28]. Since reaction-diffusion equations alone cannot describe such phenomena, a different approach is required.

The goal of this paper is to develop a hydrodynamic model suited for the description of dense colonies of bacteria growing on the surface of an agar plate, as observed in Ref. [26]. The experimental setup of Ref. [26] consists of a gel, the agar, in which nutrients are embedded, and which also contains a complex fluid, water with bacteria. A complete model of this rather complicated system would therefore require a detailed study of two different physical systems: the agar and the mixture of water and bacteria. In this paper, we focus on the latter, and only take into account basic properties of unsaturated porous media to describe the agar plate and its interaction with the fluid. Even so, the description of the mixture of water and bacteria poses a challenge of its own. Because of their size, of the order of a micron, bacteria are at the upper limit of particulate systems for which colloidal interactions are important [29]. They are also at the upper limit of particles that may exhibit Brownian motion in a fluid, since at ambient temperature and with velocity gradients estimated from the data published in Ref. [26], the Péclet number of micron-sized particles is of order 1 [30]. The point of view developed here is that hydrodynamic effects are dominant and are responsible for the whirls and jets observed in the experiment.

Hydrodynamic models involving bacteria have already been discussed in the literature. A recent model by Bees *et al.* [31] describing the swarming behavior of *Serratia liquefaciens* suggests that colony expansion is directly related to the spreading of a thin film made by a wetting agent secreted by swarmers. The situation considered here is different, since the bacteria do not produce a surfactant and swim in a thin layer at the surface of the wet agar medium. Models intended to describe pattern-forming instabilities such as bioconvection (see Refs. [32,33] and references therein) are only appropriate when bacteria are dilute in the fluid. Moreover, multiplication of bacteria is not taken into account in such models, since it is assumed that most bioconvection patterns reach their steady states quickly enough. The motion of a single bacterium in a low Reynolds number incompressible fluid is described by the Stokes equation with no-slip boundary conditions on the flagella and vanishing velocity at infinity. Under these conditions, hydrodynamic interactions between bacteria become significant when the average separation between neighboring cells is smaller than the largest physical dimension of each bacterium [34]. Since the average distance between neighboring bacteria in a dense colony growing on an agar plate is about one-third of the diameter of a bacterium, considering the bacteria together with the water in which they move as a single complex fluid is a natural approximation.

A hydrodynamic equation was proposed by Toner and Tu [35] to describe the collective motion of self-propelled particles, which have a tendency to align their speed with that of their neighbors. Such a model was introduced by Vicsek *et al.* in Ref. [36] and further studied in Ref. [37]. Collective behaviors are expected to appear in this case because the direction (angle) in which a particle moves is given by the average of the directions of motion of its nearest neighbors plus some uniformly distributed noise. As a consequence, if the noise amplitude is fixed, there is a threshold value of the particle density above which the average of the particle velocities over the whole particle ensemble is nonzero. Similarly, if the particle density is fixed, there is a threshold value of the noise amplitude below which collective motion is observed. The hydrodynamic equation proposed by Toner and Tu in Ref. [35] therefore has a Ginzburg-Landau component that describes the bifurcation of the averaged particle velocity field towards a nonzero value. It also contains a Navier-Stokes component with nonclassical inertial terms. The authors of Ref. [35] argue that such terms are permitted because the Galilean invariance is broken by the ensemble of particles.

The model we present here assumes neither the spontaneous formation of coherent structures, nor the breaking of the Galilean invariance. Following Drew [38], we consider that a mixture cannot ''know whether it is referred to an inertial frame.'' In fact, if the density of bacteria and water is constant and if bacterial collisions are neglected, the simplified hydrodynamic equation we obtain is the Navier-Stokes equation. In a quasi-two-dimensional setting, this equation has the property of transfering energy from small to large scales [39,40], and we use this mechanism of inverse energy transfer to model the spontaneous formation of whirls and jets in the colony. Our approach also provides a general framework for the use of advection-reaction-diffusion equations to model bacterial colony expansion, since the continuity equations we obtain for bacteria and water are reaction-diffusion equations with an advection term involving the water-bacteria mixture averaged velocity field.

This paper is organized as follows: experimental results of Ref. [26] are summarized in Sec. II. Section III is devoted to the presentation of the hydrodynamic model. In Sec. IV, elimination of the velocity field leads to a set of reaction-diffusion equations with a chemotaxislike term, similar to Keller and Segel's model for chemotactic organisms [16,17], but now valid for dense bacterial systems. These equations are different from the models with nonlinear diffusion and lubricating fluid reviewed in Ref. [6] or Ref. [19] but are also able to reproduce branched colonies. Moreover, they have the advantage of being based on the hydrodynamic model presented here. In Sec. V, we show numerical simulations of these equations and of the full hydrodynamic model discussed in Sec. III. Section VI is a conclusion. Appendixes are devoted to an illustration of a typical velocity field profile in a vertical cross section of the agar plate and to an explanation of how our model may be derived using a two-phase fluid approach.

II. EXPERIMENTAL RESULTS AND ORDERS OF MAGNITUDE

Whirls and jets described in Ref. [26] appeared in large (that is of diameter greater than 50 mm) colonies of *Bacillus subtilis* growing in 150-mm-diameter Petri dishes containing

soft agar. *B. subtilis* is a rodlike bacterium whose diameter is about 0.7 μm and whose length is ≈ 3 μm. It was found in Ref. [26] that local organization of the colony involved an alternation of whirls and jets: a clockwise (CW) whirl would disorganize itself into two counterpropagating jets, which would then lead to the formation of a counterclockwise (CCW) whirl. The process repeated itself in a seemingly regular fashion. Whirls were organized in a superstructure, in which neighboring whirls rotated in opposite directions. On average, whirls and jets lived for only about 0.25 s and each cycle (CW whirl–jets–CCW whirl–jets) took about 1 s to complete. The area of each whirl was ≈ 1000 μm^2 and jets had a typical length of 95 μm and a width of 12 μm. The width of each jet was therefore comparable to the radius ($\simeq 20$ μm) of whirls. The speed of cells within jets was about 100 μm s^{-1} and typical distances traveled by cells ranged between 22 μm and 30 μm. As the agar dried out, swimming ceased except in a few scattered whirls where the speed was as low as 4 μm s^{-1}. It was checked, however, that addition of water to the agar restored the swimming motion as well as the characteristic sizes of whirls and jets described above.

These numbers should be compared [26] to the typical size of a bacterium (3 μm) and to typical swimming speeds: about ten times the cell length per second [41,42]. For bacteria swimming in water (of kinematic viscosity $\nu^W \simeq 10^{-6}$ m^2 s^{-1}), and for a typical length equal to the length of a bacterium, we find a ''small-scale'' Reynolds number for bacterial swimming,

$$\mathrm{Re}^S = \frac{vL}{\nu^W} \simeq \frac{(30\times 10^{-6})(3\times 10^{-6})}{10^{-6}} \simeq 10^{-4} \ll 1.$$

In general, hydrodynamics involving bacteria is thus considered to take place at small Reynolds numbers. The situation is slightly different in the experiments described in Ref. [26], since we are clearly faced with a turbulent regime where many spatial and temporal scales coexist. In this context, the Reynolds number usually varies according to the scale at which it is defined. For instance, if we use experimentally measured bacterial speed values and take as a characteristic length the typical distance traveled by bacteria, we find a Reynolds number

$$\mathrm{Re}^B \simeq \frac{(100\times 10^{-6})(25\times 10^{-6})}{10^{-6}} = 2.5\times 10^{-3},$$

which is one order of magnitude larger than Re^S. But there are also large-scale structures observed in the experiments in which ''changes in patterns appear to be coordinated over'' thousands of microns [26]. With a characteristic length of a thousand microns, the Reynolds number is of order 1. Another approach is to try to estimate the diffusion time scale by considering the time it takes for whirls and jets to reach their characteristic sizes when water is added to a dry colony (we assume that diffusion of water is fast compared to the rate at which strain is transmitted from fluid particle to fluid particle). This gives a diffusion time $\tau_D \simeq 5$ s [26]. For a convective time, we can take the lifetime of whirls and jets, that is, $\tau_C \simeq 0.25$ s. Their ratio gives a Reynolds number based on the dynamics of whirls and jets,

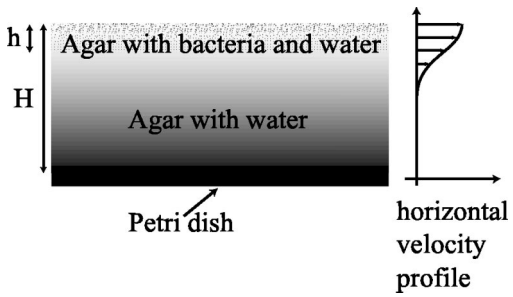

FIG. 1. Schematic of a vertical cross section of the agar plate, together with the corresponding horizontal velocity profile.

$$\mathrm{Re}^{WJ} = \frac{\tau_D}{\tau_C} \simeq \frac{5}{0.25} = 20 \gg \mathrm{Re}^S.$$

Even though Re^{WJ} may be an overestimate of the large-scale Reynolds number, the wide range of scales and associated Reynolds numbers that we have just discussed suggests that inertial effects may have to be taken into account to adequately model the experiments of [26].

Coherent structures were observed in the outer (and wetter) regions of growing colonies. The speed at which the colony boundary moved was much smaller than the bacterial velocity measured in whirls and jets, which indicates that at least two very different time scales are involved in this problem. In what follows, we present a model in which colony expansion is described by reaction-diffusion equations with advection, coupled to an equation for an averaged velocity field. The colony boundary, which is defined as a region of steep bacterial concentration gradient, is modeled by a front solution to the advection-reaction-diffusion equations. The speed at which this front moves should be small compared to the magnitude of hydrodynamic motions within the colony.

III. HYDRODYNAMIC MODEL

In this section, we write down hydrodynamic equations for a fluid that consists of densely packed bacteria and water. To build this model, we make the following general hypotheses, which are consistent with experimental conditions.

A. General setting

Figure 1 is a schematic of a vertical cross section of the growth medium, together with the corresponding horizontal velocity profile. As illustrated in this figure, we assume that the bacteria swim near (and mainly at) the surface of a porous medium, agar, which contains water. This is consistent with experimental observations [7,26]. A simple application of Brinkman's equations for porous media [43] shows that in the presence of a shear flow near the surface, the vertical velocity profile has a characteristic length that is proportional to the square root of the permeability k of the medium. More

precisely, for a steady flow and in the absence of inertial terms, the velocity field $\boldsymbol{v}^W$ of the fluid in the porous medium satisfies

$$\mathbf{0} = -\boldsymbol{\nabla} p + \mu^* \nabla^2 \boldsymbol{v}^W - \frac{\mu}{k} \boldsymbol{v}^W, \tag{1}$$

where μ is the dynamic viscosity of the fluid, μ^* is its effective viscosity, and k is the permeability of the porous medium. A divergence-free solution $\boldsymbol{v}^W(z)$ of this equation with boundary condition $\boldsymbol{v}^W(0) = v_0 \hat{\boldsymbol{x}}$ at the surface is given by

$$\boldsymbol{v}^W(z) = \left[v_0 \exp(\alpha z) - \frac{C}{\alpha^2} [1 - \exp(\alpha z)] \right] \hat{\boldsymbol{x}},$$

$$\alpha^2 = \frac{\mu}{k \mu^*}, \quad z \leqslant 0.$$

Here $\hat{\boldsymbol{x}}$ is a unit vector in the horizontal direction and the constant C is related to the horizontal pressure gradient, assumed uniform in the vertical direction, by $\boldsymbol{\nabla} p = C \mu^* \hat{\boldsymbol{x}}$. At lowest order [44], $\mu^* \simeq \mu$ and the typical penetration length is thus of order $\sqrt{k}$. As discussed in Ref. [44], the actual characteristic length depends of the geometry of the porous medium and may be as low as $\sqrt{k}/4$. If the horizontal pressure gradient is small compared to v_0, the expression for $\boldsymbol{v}^W$ shows that motion takes place in a thin layer of thickness $h_0 = O(\sqrt{k})$ near the surface of the agar plate. Since $\sqrt{k}$ is comparable to the size of a pore in the agar, h_0 is therefore much smaller than the thickness H of the agar plate.

In the situation of interest here, no shear flow is imposed at the surface and stress-free boundary conditions should be used. This more realistic setup is discussed in Appendix A, where it is shown that if the pressure gradient is nonzero in a region of thickness h near the surface, the vertical velocity profile will be fairly large up to a depth of order h and then decay exponentially with a penetration length of size $\sqrt{k}$. The existence of this finite, but small, penetration length justifies the fact that most of the motion is quasi-two-dimensional. In practice, experiments on agar plates about 10–12 mm deep reveal that cells grow about 20 μm into the agar. For thin agar slabs ($H \simeq 3$–4 mm), the cell penetration length is 8–10 μm.

Our hydrodynamic model consists of a momentum conservation equation for the velocity field of the bacteria-water mixture, coupled to three continuity equations for the concentration of water, bacteria, and nutrients in the top layer of the agar. In what follows, we first write these equations in three dimensions and then reduce them to a two-dimensional approximation by averaging over the thin vertical layer of thickness h in which fluid motions take place.

B. Continuity equation for nutrients

As food is consumed by bacteria, fresh nutrients diffuse through the agar plate. We assume that, as far as nutrients are concerned, the agar is a homogeneous isotropic medium.[1] As a consequence, diffusion of nutrients in the plate is described by Fick's law with a scalar diffusion coefficient D^S. Since the region of the agar plate where the bacteria move is thin compared to the horizontal extent of the plate, it is reasonable to assume that vertical diffusion of nutrients in this region is fast and that the concentration of nutrients is therefore independent of z in the top layer of thickness h. We also assume that the amount of nutrients at each point in the top layer is directly proportional to the concentration of nutrients in the agar plate below. In other words, we consider that $h \ll H < L^S$, where L^S is the nutrients diffusion length in the agar plate. Finally, we suppose that hydrodynamic motions of nutrients are impeded by the agar matrix and are therefore neglected. Thus, if we denote by $S(x,y,z,t)$ the concentration of nutrients in the system, S satisfies the following reaction-diffusion equation:

$$\frac{\partial S}{\partial t} = R_S + D^S \nabla^2 S, \tag{2}$$

where R_S describes nutrient consumption by the bacteria and $D^S \nabla^2 S$ describes the diffusion of S in the substrate. In Secs. IV and V, we assume $R_S = -k_0 N S$ or $R_S = -k_0 N (1+S)^2$, where N (defined below) is the mass of bacteria per unit volume.

C. Hydrodynamics of bacteria and water

We now turn to the description of fluid motions in the top part of the agar plate. We consider the mixture of bacteria and water as a very dense and viscous fluid, whose dynamics is in first approximation given by the Navier-Stokes equation. We denote by W the mass of water and by N the mass of bacteria per unit volume. We also define the ''wetness'' coefficient of the medium by

$$\delta = W/(N+W),$$

which measures the mass of water relative to the total mass of bacteria and water. A dry medium corresponds to small values of δ and a medium with no bacteria gives $\delta = 1$. The experiments described in Ref. [26] where bacteria are densely packed correspond to intermediate values of δ.

1. Continuity equations for water and bacteria

The continuity equations for N is a reaction-diffusion equation of the form

[1]This condition can, of course, be relaxed. For instance, one could envision including randomness in the flux of nutrients inside the agar.

$$\frac{\partial N}{\partial t}+\boldsymbol{\nabla}\cdot(N\boldsymbol{v})=R_N-\boldsymbol{\nabla}\cdot\boldsymbol{j}^N,$$

where R_N describes bacterial growth due to nutrient consumption and $\boldsymbol{v}$ is the velocity field of the water-bacteria mixture. The diffusion term comes from the fact that the velocity field on the left-hand side of this equation is different from the velocity field of the bacteria. In other words, the flux $\boldsymbol{j}^N$ is proportional to the velocity of bacteria relative to the mixture. If we make the hypothesis that Fick's law is valid, we get

$$\boldsymbol{j}^N=-D^N\boldsymbol{\nabla}N,$$

and if we consider D^N to be a tensor which may depend on the bacterial (N) and nutrient (S) concentrations as well as on the amount of water (W) present in the mixture, we obtain

$$\frac{\partial N}{\partial t}+\boldsymbol{\nabla}\cdot(N\boldsymbol{v})=R_N+\boldsymbol{\nabla}\cdot[D^N(N,W,S)\boldsymbol{\nabla}N]. \tag{3}$$

A similar equation can be written for W and reads

$$\frac{\partial W}{\partial t}+\boldsymbol{\nabla}\cdot(W\boldsymbol{v})=R_W(N,W,S)+\boldsymbol{\nabla}\cdot[D^W(W)\boldsymbol{\nabla}W]-\boldsymbol{\nabla}\cdot\boldsymbol{j}^W,$$

where R_W represents water evaporation[2] and $\boldsymbol{j}^W$ is the flux of water relative to the water-bacteria mixture. The term $\boldsymbol{\nabla}\cdot(D^W\boldsymbol{\nabla}W)$ describes dispersion [45] in the porous medium. Dispersion (or capillary dispersivity) of a fluid in a porous medium takes place when the latter is not saturated by the fluid [46]; since water concentration may vary throughout the agar plate, this effect should be taken into account in our model. We will assume dispersion to be isotropic and independent of the water velocity field. Note that bacteria are too big to move by capillarity, so dispersion is not included in the equation for N. Since the velocity field of the water-bacteria mixture is a mass-weighted average of the velocity fields for the water and the bacteria, the flux $\boldsymbol{j}^W$ is opposite to $\boldsymbol{j}^N$ and the equation for W therefore reads

$$\frac{\partial W}{\partial t}+\boldsymbol{\nabla}\cdot(W\boldsymbol{v})=R_W(N,W,S)+\boldsymbol{\nabla}\cdot[D^W(W)\boldsymbol{\nabla}W]-\boldsymbol{\nabla}\cdot[D^N(N,W,S)\boldsymbol{\nabla}N]. \tag{4}$$

Further details can be found in Appendix B, where these equations are obtained through a two-phase fluid description of the water-bacteria mixture.

2. Momentum conservation equation

The equation for the conservation of linear momentum of the mixture is, at lowest order, the Navier-Stokes equation

$$\rho\frac{\partial\boldsymbol{v}}{\partial t}+\rho(\boldsymbol{v}\cdot\boldsymbol{\nabla})\boldsymbol{v}=\boldsymbol{\nabla}\cdot\boldsymbol{T}+\boldsymbol{F}, \tag{5}$$

where $\rho=N+W$, $\boldsymbol{\nabla}\cdot\boldsymbol{T}$ is a stress tensor and $\boldsymbol{F}$ represents the sum of external forces exerted on a fluid particle. In what follows, we consider that the bacteria-water mixture behaves as a Newtonian fluid. The numerical simulations of Sec. V B show that many qualitative aspects of bacterial colony dynamics can be obtained within this simple approximation. Since the goal of this paper is to show how reaction-diffusion equations can be combined with hydrodynamics to describe the evolution of bacterial colony shapes as well as complex bacterial dynamics within a colony, including nonlinear effects such as viscoelasticity is beyond the scope of this work. We therefore assume that

$$\boldsymbol{\nabla}\cdot\boldsymbol{T}=-\boldsymbol{\nabla}p+\mu\nabla^2\boldsymbol{v}+\lambda\boldsymbol{\nabla}(\boldsymbol{\nabla}\cdot\boldsymbol{v}),$$

where μ is the dynamic viscosity of the mixture and λ is a second viscosity. We expect the mixture of bacteria and water to behave as an almost incompressible fluid, so the last term in the above equation will remain small. The force $\boldsymbol{F}$ contains a friction term $\boldsymbol{F}_s=-\alpha\boldsymbol{v}$ due to the interaction between the fluid and the agar matrix, bulk forces such as gravity, and a "bacterial activity" term $\boldsymbol{F}_g$ that represents subgrid scale dynamics due to flagella activity. We consider that because bacteria are living organisms, their consumption of food leads to a source term in the hydrodynamic equation (see also Ref. [28]), which we model as a small-scale random forcing $\boldsymbol{F}_g$.

3. Pressure terms

The pressure p in the expression for $\boldsymbol{\nabla}\cdot\boldsymbol{T}$ is the sum of the water and bacterial pressures p^W and p^N. Whereas p^W is the hydrodynamic pressure for an incompressible fluid, the pressure p^N needs to be related to the bacterial density N through an equation of state. This implies that p^N is locally defined, whereas p^W is a nonlocal function of the water velocity field $\boldsymbol{v}^W$, such that $\boldsymbol{\nabla}\cdot\boldsymbol{v}^W=0$. It is therefore natural to decompose the velocity field $\boldsymbol{v}$ into a component $\boldsymbol{v}^C$ driven by bacterial collisions and a hydrodynamic component $\boldsymbol{v}^H$, which remains divergence free. This decomposition does not necessarily coincide with the separation of $\boldsymbol{v}$ into its compressible and solenoidal components, since $\boldsymbol{v}^C$ may also have a divergence-free part. We will write an evolution equation for $\boldsymbol{v}^C$, which is driven by local variations of p^N (more precisely by local variations of p_c^N defined below) and determine $p^I\equiv p^W+p^N-p_c^N$ by imposing that $\boldsymbol{\nabla}\cdot\boldsymbol{v}^H$ remains equal to zero. This procedure will be implemented in Sec. III E in the case of a two-dimensional reduction of our model for a Newtonian fluid.

We now discuss the physical origin of the compressible part of the bacterial velocity field $\boldsymbol{v}^N$. One should imagine a fluid made only of bacteria. In such a fluid, the pressure p^N is a function of the density N and of the temperature T. The virial expansion for p^N is of the form [47]

$$p^N=kT[N+B_2(T)N^2+O(N^3)], \tag{6}$$

[2]Consumption of water by the bacteria could also be included in R_N and R_W.

where k is Boltzmann's constant and $B_2(T)$ is the second virial coefficient. For most gases and compressible liquids, the pressure is typically linear in the density. We expect the pressure of a fluid of dead bacteria to be described by such a linear equation. The quadratic term in Eq. (6) is important when binary collisions cannot be neglected. It is observed that live bacteria undergo many such binary collisions, which suggests that the effective temperature of a collection of living cells is higher than if they were dead. This is supported by the results of Wu and Libchaber [27], who measured the effective temperature of a "bacterial bath" of *E. coli* in a soap film, and found a temperature of the order of a hundred times the room temperature. In what follows, we consider that the linear term in N is at the origin of a quasi-incompressible behavior of the bacterial fluid and is therefore separated from the corrections proportional to N^2. In other words, we write

$$p^N = p_0^N + p_c^N, \quad \text{where} \quad p_c^N = \gamma(S,N,W)N^2.$$

It is reasonable to assume that $\gamma(S,0,W)>0$. At order N^2, the pressure term p_c^N therefore gives rise to a force which drives bacteria away from "overcrowded" regions. This process is faster than bacterial diffusion [see Eq. (3)], which describes individual random motion. Moreover, it only takes place when bacteria are alive and close to each other. It is shown in Sec. IV that when coupled to nutrient consumption, this process has, at least for short times, an effect analogous to classical chemotaxis. More precisely, bacteria tend to move towards fresh nutrients. The existence of such a phenomenon is particularly interesting here since it seems difficult to envision how classical chemotaxis can explain colony expansion towards fresh nutrients when the latter are in large supply and when bacteria are packed in a dense layer.

To summarize, our hydrodynamic model reads

$$\frac{\partial S}{\partial t} = R_S(N,W,S) + D^S \nabla^2 S,$$

$$\frac{\partial W}{\partial t} + \boldsymbol{\nabla}\cdot(W\boldsymbol{v}) = R_W(N,W,S) + \boldsymbol{\nabla}\cdot[D^W(W)\boldsymbol{\nabla}W - D^N(N,W,S)\boldsymbol{\nabla}N],$$

$$\frac{\partial N}{\partial t} + \boldsymbol{\nabla}\cdot(N\boldsymbol{v}) = R_N(N,W,S) + \boldsymbol{\nabla}\cdot[D^N(N,W,S)\boldsymbol{\nabla}N],$$

$$\frac{\partial \boldsymbol{v}}{\partial t} + (\boldsymbol{v}\cdot\boldsymbol{\nabla})\boldsymbol{v} = \frac{1}{N+W}[\boldsymbol{\nabla}\cdot\boldsymbol{T} + \boldsymbol{F}_s(N,W,\boldsymbol{v}) + \boldsymbol{F}_e + \boldsymbol{F}_g(N,W,S,v)], \tag{7}$$

where $\boldsymbol{F}_e$ represents external forces and where we made explicit the dependence of R_S, R_N, R_W, D^N, D^W, $\boldsymbol{F}_s = -\alpha(N,W)\boldsymbol{v}$, and $\boldsymbol{F}_g$ on N, W, S, and $\boldsymbol{v}$. For clarity, these dependences will be implicit in what follows. With appropriate boundary conditions and expressions for $\boldsymbol{T}$, these equations describe bacterial dynamics in regions of nonuniform wetness.

D. Two-dimensional reduction

Given the small thickness of the layer in which fluid motion takes place (see Fig. 1), it is appropriate to reduce the three-dimensional model (7) to a two-dimensional one. We already mentioned that it is reasonable to assume that W and S do not depend on the vertical coordinate. We also consider that the vertical variations of N in the thin layer of thickness h are small. The velocity field $\boldsymbol{v}$ however varies strongly in the vertical direction, as discussed in Sec. III A. At the top surface it is natural to assume stress-free boundary conditions for the velocity, while at the bottom of the agar plate we should enforce a no-slip boundary condition. From a practical point of view the depth at which the latter boundary condition is enforced is irrelevant as long as it is larger than a few multiples of h. One may expand the velocity field $\boldsymbol{v}$ on a Galerkin basis consisting of vertical profiles $f_i(z)$ satisfying the appropriate boundary conditions, as $\boldsymbol{v}(x,y,z,t) = \Sigma_i \boldsymbol{u}_i(x,y,t) f_i(z)$. Projecting the momentum equations on this basis leads to two-dimensional equations for the velocity components $u_i(x,y,t)$. A two-dimensional reduction in terms of a single horizontal velocity field is possible if a decomposition of the form $\boldsymbol{v}(x,y,z,t) = f(z)\boldsymbol{u}(x,y,t)$ is a valid approximation. It is then important to find the most appropriate profile $f(z)$. The calculation of $f(z)$ is illustrated in Appendix A in a simple case. We also assume that the vertical component of the velocity field is negligible in the top layer. Microscope observations of the colony indeed show that bacteria stay in the plane of focus for a long time, indicating very little vertical displacement. By substituting this decomposition ansatz into Eqs. (7) written for a Newtonian fluid and by integrating in the vertical direction over the depth h of the layer where most of the activity takes place, we obtain

$$\frac{\partial S}{\partial t} = R_S + D^S \nabla_h^2 S,$$

$$\frac{\partial W}{\partial t} + \boldsymbol{\nabla}_h\cdot(W\overline{\boldsymbol{v}}) = R_W + \boldsymbol{\nabla}_h\cdot(D^W\boldsymbol{\nabla}_h W - D^N\boldsymbol{\nabla}_h N),$$

$$\frac{\partial N}{\partial t} + \boldsymbol{\nabla}_h\cdot(N\overline{\boldsymbol{v}}) = R_N + \boldsymbol{\nabla}_h\cdot(D^N\boldsymbol{\nabla}_h N),$$

$$\frac{\partial \overline{\boldsymbol{v}}}{\partial t} + \zeta(\overline{\boldsymbol{v}}\cdot\boldsymbol{\nabla}_h)\overline{\boldsymbol{v}} = \frac{1}{N+W}[-\boldsymbol{\nabla}_h\overline{p} + \mu\nabla_h^2\overline{\boldsymbol{v}} + \lambda\boldsymbol{\nabla}_h(\boldsymbol{\nabla}_h\cdot\overline{\boldsymbol{v}}) - \eta\overline{\boldsymbol{v}} + \overline{\boldsymbol{F}}_e + \overline{\boldsymbol{F}}_g], \tag{8}$$

where $\overline{\boldsymbol{v}}(x,y,t) = \langle f\rangle \boldsymbol{u}(x,y,t)$ is the vertically averaged horizontal velocity, $\overline{p} = \langle p\rangle$, $\boldsymbol{\nabla}_h$ is the gradient in the horizontal direction,

$$\zeta=\frac{\langle f^2\rangle}{\langle f\rangle^2},\quad \eta=\alpha-\mu\frac{\langle d^2f/dz^2\rangle}{\langle f\rangle},$$

$$\langle g\rangle=\frac{1}{h}\left(\int_{-h}^{0}g(z)dz\right),$$

and g is any function of z. Vertical averaging is a standard procedure for thin films, usually described by linear equations, and for shallow water models, for which vertical profiles are constant. In the situation considered here, nonlinear effects are not negligible and as a consequence, the nonlinear term is renormalized by the coefficient ζ. The latter depends on the vertical profile of the velocity field and on the depth over which averaging is performed. In Appendix A, we show that the profile given by Brinkman's equations in the presence of a pressure gradient supported near the top layer is such that $\zeta\simeq 1$ as long as the averaging is performed over a distance comparable to the depth over which the pressure gradient is supported. In what follows, ζ will therefore be taken equal to 1, the bars will be dropped, and all gradients will implicitly be horizontal gradients.

E. Separation between the expansion-driven and hydrodynamic components of the flow

The momentum equation in system (8) reads

$$\frac{\partial \boldsymbol{v}}{\partial t}+(\boldsymbol{v}\cdot\boldsymbol{\nabla})\boldsymbol{v}=\frac{1}{\rho}[-\boldsymbol{\nabla}p+\mathcal{D}\boldsymbol{v}-\eta\boldsymbol{v}+\boldsymbol{F}],\tag{9}$$

where $p=p^W+p^N$, $\mathcal{D}\boldsymbol{v}=\mu\nabla^2\boldsymbol{v}+\lambda\boldsymbol{\nabla}(\boldsymbol{\nabla}\cdot\boldsymbol{v})$, and $\boldsymbol{F}=\boldsymbol{F}_e+\boldsymbol{F}_g$. As discussed in Sec. III C 3, we now decompose the velocity field $\boldsymbol{v}$ into a component $\boldsymbol{v}^C$ driven by bacterial collisions and a hydrodynamic component $\boldsymbol{v}^H$, which satisfies $\boldsymbol{\nabla}\cdot\boldsymbol{v}^H=0$. The evolution equation for $\boldsymbol{v}^C=\boldsymbol{v}-\boldsymbol{v}^H$ is defined as

$$\frac{\partial \boldsymbol{v}^C}{\partial t}=-\frac{1}{\rho}\boldsymbol{\nabla}p_c^N+\frac{1}{\rho_m}\mathcal{D}\boldsymbol{v}^C-\frac{\eta_m}{\rho_m}\boldsymbol{v}^C,\tag{10}$$

where η_m and ρ_m are typical (constant) values of η and ρ in the system. This equation is linear in $\boldsymbol{v}^C$, which allows us to obtain a single equation for $\boldsymbol{v}$, Eq. (11), as shown below. Substracting Eq. (10) from Eq. (9), the equation for $\boldsymbol{v}^H$ reads

$$\frac{\partial \boldsymbol{v}^H}{\partial t}=-(\boldsymbol{v}\cdot\boldsymbol{\nabla})\boldsymbol{v}-\frac{1}{\rho_m}\mathcal{D}\boldsymbol{v}^C+\frac{\eta_m}{\rho_m}\boldsymbol{v}^C+\frac{1}{\rho}[-\boldsymbol{\nabla}p^I+\mathcal{D}\boldsymbol{v}-\eta\boldsymbol{v}+\boldsymbol{F}].$$

The pressure $p^I=p-p_c^N=p^W+p_0^N$ is obtained from the condition $\boldsymbol{\nabla}\cdot\boldsymbol{v}^H=0$ for all times. The definitions of $\boldsymbol{v}^C$ and p^I satisfy the following criteria: when bacterial collisions dominate the dynamics (i.e., if $\boldsymbol{\nabla}p_c^N\neq\boldsymbol{0}$ and if the forcing is negligible), the velocity field is mostly compressible and should be close to $\boldsymbol{v}^C$; when hydrodynamic motions take place, $\boldsymbol{v}$ should be mostly incompressible (since $\boldsymbol{v}\simeq\boldsymbol{v}^W$ and $\boldsymbol{\nabla}\cdot\boldsymbol{v}^W=0$) and close to $\boldsymbol{v}^H$. The definition of p^I ensures that these conditions are satisfied. The equation for $\boldsymbol{v}^H$ can be rewritten as

$$\frac{\partial \boldsymbol{v}^H}{\partial t}=-(\boldsymbol{v}\cdot\boldsymbol{\nabla})\boldsymbol{v}-\frac{\boldsymbol{\nabla}p^I}{\rho}+\left(\frac{1}{\rho}-\frac{1}{\rho_m}\right)(\mathcal{D}\boldsymbol{v}^C+\mathcal{D}\boldsymbol{v}^H)+\frac{1}{\rho_m}\mathcal{D}\boldsymbol{v}^H-\frac{\eta}{\rho}(\boldsymbol{v}^C+\boldsymbol{v}^H)+\frac{\eta_m}{\rho_m}\boldsymbol{v}^C+\frac{\boldsymbol{F}}{\rho}.$$

The condition $\boldsymbol{\nabla}\cdot\boldsymbol{v}^H=0$ leads to an equation for p^I, which may be difficult to solve, especially if the boundary conditions are not periodic [48]. Here, since $\boldsymbol{v}$ vanishes outside the colony, one can use periodic boundary conditions with a box whose size is larger than that of the colony. As a consequence, the above equation may be replaced by

$$\begin{aligned}\frac{\partial \boldsymbol{v}^H}{\partial t}&=\mathcal{P}\left[-(\boldsymbol{v}\cdot\boldsymbol{\nabla})\boldsymbol{v}+\left(\frac{1}{\rho}-\frac{1}{\rho_m}\right)\mathcal{D}\boldsymbol{v}+\frac{1}{\rho_m}\mathcal{D}\boldsymbol{v}^H-\left(\frac{\eta}{\rho}-\frac{\eta_m}{\rho_m}\right)\boldsymbol{v}-\frac{\eta_m}{\rho_m}\boldsymbol{v}^H+\frac{\boldsymbol{F}}{\rho}\right]\\&=\mathcal{P}\left[-(\boldsymbol{v}\cdot\boldsymbol{\nabla})\boldsymbol{v}+\left(\frac{1}{\rho}-\frac{1}{\rho_m}\right)\mathcal{D}\boldsymbol{v}-\left(\frac{\eta}{\rho}-\frac{\eta_m}{\rho_m}\right)\boldsymbol{v}+\frac{\boldsymbol{F}}{\rho}\right]+\frac{1}{\rho_m}\mathcal{D}\boldsymbol{v}^H-\frac{\eta_m}{\rho_m}\boldsymbol{v}^H,\end{aligned}$$

where $\mathcal{P}\boldsymbol{v}$ is the projection of $\boldsymbol{v}$ on its solenoidal part. With periodic boundary conditions, $\mathcal{P}$ is uniquely defined by $\mathcal{P}\boldsymbol{v}=\boldsymbol{\nabla}\times\boldsymbol{v}_S$, where $\boldsymbol{v}=\boldsymbol{\nabla}\times\boldsymbol{v}_S+\boldsymbol{\nabla}V$. Moreover, this projection can easily be performed in Fourier space. In the above equations, we used the fact that $\mathcal{P}\mathcal{D}\boldsymbol{v}^H=\mathcal{D}\mathcal{P}\boldsymbol{v}^H=\mathcal{D}\boldsymbol{v}^H$, since $\boldsymbol{v}^H$ is solenoidal. Initial conditions for $\boldsymbol{v}^H$ are such that $\boldsymbol{v}^H=\boldsymbol{0}$ and since $\boldsymbol{\nabla}\cdot\boldsymbol{v}^H$ is conserved by the above equation, $\boldsymbol{v}^H$ remains solenoidal. The dynamic equation for $\boldsymbol{v}=\boldsymbol{v}^C+\boldsymbol{v}^H$ is then

$$\begin{aligned}\frac{\partial \boldsymbol{v}}{\partial t}&=\mathcal{P}\left[-(\boldsymbol{v}\cdot\boldsymbol{\nabla})\boldsymbol{v}+\left(\frac{1}{\rho}-\frac{1}{\rho_m}\right)\mathcal{D}\boldsymbol{v}-\left(\frac{\eta}{\rho}-\frac{\eta_m}{\rho_m}\right)\boldsymbol{v}+\frac{\boldsymbol{F}}{\rho}\right]\\&\quad-\frac{1}{\rho}\boldsymbol{\nabla}p_c^N+\frac{1}{\rho_m}\mathcal{D}\boldsymbol{v}-\frac{\eta_m}{\rho_m}\boldsymbol{v}.\end{aligned}\tag{11}$$

With $\boldsymbol{F}=\boldsymbol{0}$, the velocity field $\boldsymbol{v}^H$ is expected to remain small as long as $\boldsymbol{v}^C$ and $\mathcal{D}\boldsymbol{v}^C$ are small. Our full hydrodynamic model then reads

$$\frac{\partial S}{\partial t}=R_S+D^S\nabla^2S,$$

$$\frac{\partial W}{\partial t}+\boldsymbol{\nabla}\cdot(W\boldsymbol{v})=R_W+\boldsymbol{\nabla}\cdot(D^W\boldsymbol{\nabla}W)-\boldsymbol{\nabla}\cdot(D^N\boldsymbol{\nabla}N),$$

$$\frac{\partial N}{\partial t}+\boldsymbol{\nabla}\cdot(N\boldsymbol{v})=R_N+\boldsymbol{\nabla}\cdot(D^N\boldsymbol{\nabla}N),$$

$$\frac{\partial \boldsymbol{v}}{\partial t}=\mathcal{P}\left[-(\boldsymbol{v}\cdot\boldsymbol{\nabla})\boldsymbol{v}+\left(\frac{1}{\rho}-\frac{1}{\rho_m}\right)\mathcal{D}\boldsymbol{v}-\left(\frac{\eta}{\rho}-\frac{\eta_m}{\rho_m}\right)\boldsymbol{v}+\frac{\boldsymbol{F}}{\rho}\right]$$
$$-\frac{1}{\rho}\boldsymbol{\nabla}p_c^N+\frac{\mathcal{D}\boldsymbol{v}}{\rho_m}-\frac{\eta_m}{\rho_m}\boldsymbol{v} \qquad (12)$$

for a Newtonian fluid, i.e., with $\mathcal{D}\boldsymbol{v}=\mu\nabla^2\boldsymbol{v}+\lambda\boldsymbol{\nabla}(\boldsymbol{\nabla}\cdot\boldsymbol{v})$. The force $\boldsymbol{F}$ is given by $\boldsymbol{F}=\boldsymbol{F}_e+\boldsymbol{F}_g$. Again, $\boldsymbol{F}_e$ corresponds to changes in linear momentum due to external forces and $\boldsymbol{F}_g$ describes changes in linear momentum due to bacterial activity.

The rest of this paper is devoted to a discussion of some basic properties of the hydrodynamic model (12). In Sec. IV, we investigate the role of the nonlinear term in the equation for the bacterial pressure p^N and show that when this term is dominant, collective motion of the colony towards fresh nutrients is expected. In this case, Eqs. (12) have a singular limit in the form of a set of advection-reaction-diffusion equations, the behavior of which is then illustrated in the numerical simulations of Sec. V. The advection term in these equations is proportional to the gradients of S, and therefore leads to collective behaviors similar to classical chemotaxis. The role of water in these equations is also analyzed. At the end of Sec. V, we present simulations of the complete hydrodynamic model (12) and show that coherent structures in the form of whirls and jets are obtained when the small-scale forcing $\boldsymbol{F}_g$ is finite.

IV. EXPANSION-DRIVEN DYNAMICS

A. Chemotacticlike behavior

In 1971, Keller and Segel [16,17] proposed a simple model for the chemotactic behavior of motile bacteria swimming in a fluid in the presence of a gradient of nutrients. Conservation of bacteria and nutrients was described in terms of two advection-diffusion equations, where the advection term in the equation for N was of the form $\boldsymbol{\nabla}\cdot[N\chi(S)\boldsymbol{\nabla}S]$. The coefficient $\chi(S)$ was called ''chemotactic coefficient.'' A similar model may be recovered from our general hydrodynamic equations if we eliminate the velocity field $\boldsymbol{v}$ from Eqs. (12). We indeed have

$$\frac{\partial S}{\partial t}=R_S+D^S\nabla^2S,$$

$$\frac{\partial W}{\partial t}+\boldsymbol{\nabla}\cdot(W\boldsymbol{v})=R_W+\boldsymbol{\nabla}\cdot(D^W\boldsymbol{\nabla}W)-\boldsymbol{\nabla}\cdot(D^N\boldsymbol{\nabla}N),$$

$$\frac{\partial N}{\partial t}+\boldsymbol{\nabla}\cdot(N\boldsymbol{v})=R_N+\boldsymbol{\nabla}\cdot(D^N\boldsymbol{\nabla}N), \qquad (13)$$

where, R_N models bacterial growth due to nutrient consumption, R_W accounts for water loss, and R_S describes nutrient consumption by bacteria. This system is in closed form if $\boldsymbol{v}$ is a function of N, W, and S. It indicates that, as bacteria are advected at the mean velocity $\boldsymbol{v}$, their mass changes by diffusion and by growth due to nutrient consumption; nutrients diffuse in the substrate and are consumed by bacteria. Note that Eq. (3) was written with the assumption that D^N vanishes when $W=0$, which is necessary if one wants $W=0$ to be a solution of Eqs. (13).

We now obtain an expression for $\boldsymbol{v}$ of the form $\chi(S)\boldsymbol{\nabla}S$ as an illustration of the role of the term γN^2 in the expression for the bacterial pressure p^N. We first assume that nutrient dynamics is dominated by the reaction term R_S, i.e., neglect diffusion in the continuity equation for S. With $R_S=-k_0Nf(S)$, where, for instance, $f(S)=S$ as in Ref. [17] or $f(S)=(1+S)^2$ as in Ref. [49], and in the absence of diffusion [17], Eq. (2) reads

$$N=-\frac{1}{k_0}\frac{\partial G(S)}{\partial t}, \quad \text{where} \quad G(S)=\int\frac{dS}{f(S)}.$$

Dropping all but the expansion term on the right-hand side of Eq. (9), neglecting the nonlinear terms and assuming that γ is a constant, we obtain

$$\rho\frac{\partial \boldsymbol{v}}{\partial t}=-\gamma\boldsymbol{\nabla}(N^2)=-2\gamma N\boldsymbol{\nabla}N,$$

i.e.,

$$\frac{\partial \boldsymbol{v}}{\partial t}=-2\gamma\frac{N}{\rho}\boldsymbol{\nabla}N=2\gamma\frac{N}{\rho}\boldsymbol{\nabla}\left(\frac{1}{k_0}\frac{\partial G(S)}{\partial t}\right)=\frac{2\gamma}{k_0}\frac{N}{\rho}\frac{\partial\boldsymbol{\nabla}G(S)}{\partial t},$$

which, after integrating over time (assuming that temporal derivatives of N/ρ are negligible), gives

$$\boldsymbol{v}\simeq\frac{2\gamma}{k_0}\frac{N}{\rho}\frac{\boldsymbol{\nabla}S}{f(S)}=\chi(N,W,S)\boldsymbol{\nabla}S\equiv\boldsymbol{v}^{chem}, \qquad (14)$$

where

$$\chi(N,W,S)=2\frac{\gamma}{k_0}\frac{N}{\rho}\frac{1}{f(S)}.$$

The expressions of R_S and $\chi(N,W,S)$ are therefore related to each other through the expansion term (γN^2) in the momentum equation (9). If $N/\rho\simeq1$ and $f(S)=S$, we obtain a term similar to Keller and Segel's [17] chemotactic coefficient $\chi(S)=2(\gamma/k_0)(1/S)$. With $f(S)=(1+S)^2$, we obtain $\chi(S)=2(\gamma/k_0)[1/(1+S)^2]$, which is also observed in chemotaxis experiments [50].

It is important to realize that the chemotactic limit we have just discussed may not be regular (i.e., that the solution to the hydrodynamic equation with small inertial, pressure, and diffusive terms may not be a small perturbation of the solution of the hydrodynamic equation with these terms set to zero). In particular, the velocity field $\boldsymbol{v}=\chi(N,W,S)\boldsymbol{\nabla}S$ breaks the approximation that $\boldsymbol{v}$ should be almost solenoidal.

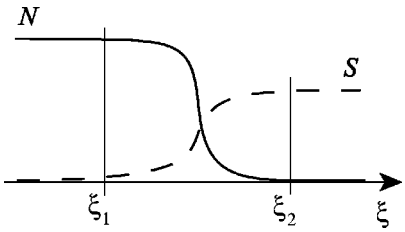

FIG. 2. Sketch of the profiles of N and S in a direction perpendicular to the colony boundary.

Moreover, the assumption that N/ρ is constant in time, which was made to obtain a simple expression for $\boldsymbol{v}$ will not be preserved by these equations, unless W is small. In Sec. V B 1, we provide a numerical comparison of the full hydrodynamic model with the advection-reaction-diffusion equations given by Eqs. (13) and (14). We show that the limit discussed here is indeed singular but that the advection-reaction-diffusion model gives qualitatively good results, even at large times. Equations (13) and (14) represent an advection-reaction-diffusion model for the growth of bacterial colonies. Together with bacterial and nutrient concentrations, this model involves a third variable, water, which plays a role similar to the wetting agents or lubricants produced by some bacterial strains [4,6,10]. This is illustrated in the following section, where some properties of W are discussed.

B. Bacteria-water interaction

Let us consider a colony with a straight boundary, moving at a uniform speed c. If we denote by x the coordinate in the direction transverse to the boundary and if we place ourselves in the frame moving at speed c, the equation for W becomes

$$\frac{\partial W}{\partial t}-c\frac{\partial W}{\partial \xi}+\frac{\partial (Wv)}{\partial \xi}=R_W+\frac{\partial}{\partial \xi}\left(D^W\frac{\partial W}{\partial \xi}\right)-\frac{\partial}{\partial \xi}\left(D^N\frac{\partial N}{\partial \xi}\right),$$

where $\xi=x-ct$. The last term on the right-hand side of this equation is a flux in the direction of the gradients of N, that is, towards the inside of the colony. One can understand this at a microscopic level: bacteria going down the gradients of N are replaced by water as they move.

Let us assume that N and S have profiles as sketched in Fig. 2, and that $R_W=0$. Let ξ_1 and ξ_2 be the coordinates in the moving frame of two points on each side of the front and let us integrate the above equation between ξ_1 and ξ_2. We obtain

$$\begin{aligned}Q\equiv\frac{d}{dt}\int_{\xi_1}^{\xi_2}W(\xi)d\xi=&c[W(\xi_2)-W(\xi_1)]+W(\xi_1)v(\xi_1)\\&-W(\xi_2)v(\xi_2)+[D^W(\xi_2)W_\xi(\xi_2)-D^W(\xi_1)W_\xi(\xi_1)]\\&-[D^N(\xi_2)N_\xi(\xi_2)-D^N(\xi_1)N_\xi(\xi_1)],\end{aligned}$$

where $D^{N,W}(\xi)=D^{N,W}(N(\xi),W(\xi),S(\xi))$ and W_ξ and N_ξ stand for the derivatives with respect to ξ of W and N, respectively. Since the velocity

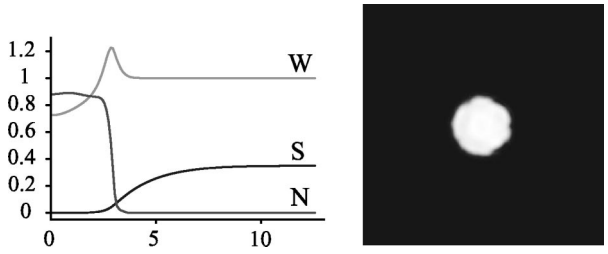

FIG. 3. Numerical solution of Eqs. (13) and (14) at $t=80$. The parameters are $D^N=0.05(1+\sigma)NS$, where σ is a random number with a triangular distribution of support $[-1,1]$, $R_S=-NS$, $R_N=NS$, $R_W=0$, $k_0=1$, $\gamma=0.01$, $D^S=0.1$, and $D^W=0.005$. Left: profiles of N, S, and W as functions of position, along a horizontal half-line going through the middle of the colony. Right: gray-scale picture of N as a function of space.

$$v(\xi)=\frac{2\gamma}{k_0}\frac{N(\xi)}{W(\xi)+N(\xi)}\frac{S_\xi}{f(S(\xi))}$$

is proportional to N, we can consider that $v(\xi_2)\simeq 0$, if ξ_2 is chosen far enough from the front solution (see Fig. 2). By choosing ξ_1 in a similar way, we can neglect $W_\xi(\xi_1)$, $W_\xi(\xi_2)$, $N_\xi(\xi_1)$, and $N_\xi(\xi_2)$, so that

$$Q\equiv\frac{d}{dt}\int_{\xi_1}^{\xi_2}W(\xi)d\xi\simeq c[W(\xi_2)-W(\xi_1)]+W(\xi_1)v(\xi_1).$$

Moreover, $v(\xi_1)>0$. If we start from a situation where W is homogeneous, then Q is positive due to a flux of water through the line $\xi=\xi_1$. As a consequence, we expect $W(\xi_1)$ to become less than $W(\xi_2)$, which also increases the amount of water present near the front of the colony. This mechanism can saturate either by including evaporation into the model (i.e., by setting $R_W=-\lambda W$ where $\lambda>0$), or if one of the terms neglected above becomes large. Also note that for $v(\xi_1)$ to be significantly large, one needs $S_\xi(\xi_1)$ finite, which implies that the diffusion length of the nutrients is larger than that of N and W.

This argument indicates that if the above conditions hold, one expects W to be relatively large near the boundary of the colony. From a physical point of view, bacteria moving towards fresh nutrients drag the water along so that water is depleted inside the colony. This effect is counteracted by the diffusion term in the equation for W. From a biological point of view, an increased amount of water will help bacteria swim and will therefore favor colony expansion. From a modeling point of view, W plays a role similar to the lubricant [6,10] or wetting agent [4] secreted by some bacterial strains to sustain bacterial motion. Figure 3 shows a solution to Eqs. (13) at time $t=80$. The shape of the colony can be seen from the gray-scale picture of N as a function of space, shown on the right. On the left side of the figure, the profiles of N, S, and W are plotted along a horizontal half-line going through the middle of the colony. In this run, the maximum of W increases as a function of time until the gradients of S behind the front become too small. Note that the gradients of W are not small behind the front, which also provides a mechanism to reduce the value of Q. Experimental observa-

tions confirm that the region just behind the colony boundary is much wetter than the agar in front of it.

V. NUMERICAL SIMULATIONS

We start this section with numerical simulations of the advection-reaction-diffusion equations introduced in Sec. IV. We then turn to the full two-dimensional hydrodynamic system written for a Newtonian fluid and illustrate the chemotactic and hydrodynamic limits of this model. The simulations shown below illustrate a few properties of Eqs. (12) and (13) but are by no means the result of a complete exploration of these models. Such a discussion is beyond the scope of this paper and will be published separately.

Numerical integration is performed in a box of size 8π with periodic boundary conditions, using a Fourier pseudospectral method. For the reaction-diffusion model, linear terms are integrated exactly and nonlinear terms are integrated with an Adams-Bashforth scheme. For the full hydrodynamic model, the time stepping is based on a Crank-Nicholson scheme for the linear part of the viscous and diffusion terms and on an Adams-Bashforth scheme for the nonlinear terms. The use of this scheme is preferred over a low-storage third-order Runge-Kutta scheme because for the latter the time steps required to keep numerical dissipation smaller than physical dissipation are prohibitively small. It is interesting to note that when acting on a solenoidal field $\boldsymbol{v}$, the Crank-Nicholson scheme only preserves the divergence-free character of $\boldsymbol{v}$ when the linear viscous term $(1/\rho_m)[\mu\nabla^2\boldsymbol{v}+\lambda\boldsymbol{\nabla}(\boldsymbol{\nabla}\cdot\boldsymbol{v})]$ is such that $\lambda=\mu/3$, i.e., when the bulk viscosity is zero. All simulations are performed with a spatial resolution of 256^2 grid points in the reaction-diffusion case and of 512^2 in the case of the full hydrodynamic model. The time step is 0.1 in all cases.

A. Advection-reaction-diffusion model

There is extensive literature on the fingering instability of interfaces (see, for instance, Refs. [51,52]), in particular, in the case of reaction-diffusion systems [53–55], or in situations where hydrodynamic phenomena such as viscous fingering or Rayleigh-Taylor instabilities are coupled to reaction-diffusion equations [56–58]. In what follows, we give a brief summary of reaction-diffusion models that have been proposed to describe bacterial colony shapes (for a review, see, for instance, Refs. [6,19]). We then present simulations of our model with similar reaction and diffusion terms. For $W=0$, $R_N=-R_S=NS$, and D^N and D^S constant, Kessler and Levine [59] showed that in order for the front solution representing the colony boundary to become unstable, the reaction term R_N should be set to zero if N is below some threshold value, which depends on the ratio D^N/D^S. This is sufficient to destabilize the colony boundary but not to produce branches. By adding a bacterial ''death'' term to R_N, Golding *et al.* [6] indicated that thick branches could be obtained [the colony is then formed by active and inactive (or ''dead'') bacteria]. Earlier, Kitsunezaki [60] had proposed a model with bacterial decay (or death) and nonlinear diffusion, which produced dendriticlike structures. His simulations were performed on a random lattice, and it turns out that randomness is essential in his model. We have indeed checked that by refining the mesh size, the instability giving rise to fine structures on a *regular* lattice disappears; this was also noticed by Mimura *et al.* [19]. Kawasaki *et al.* [61] proposed to use a stochastic nonlinear diffusion coefficient in the equation for N to account for agar inhomogeneity. In this case, dendriticlike colony shapes can be reproduced, even in the absence of the bacterial depletion term introduced by Kitsunezaki or Golding *et al.* More recently, Mimura *et al.* [19] proposed a model that involves a piecewise continuous death term and a (nonstochastic) nonlinear piecewise continuous diffusion coefficient in the equation for N. This model captures a variety of colony shapes when its parameters are varied. As mentioned before, Golding *et al.* [6] introduced a model with lubricant, which can also reproduce most of the colony shapes observed in the experiments. To our knowledge, no rigorous analysis of the nature of the instability leading to branched colony shapes in these models has been performed, except in the simplest case [59]. It would be extremely interesting to determine the exact role played by the reaction and diffusion terms in the development of branched structures for more complex models, in particular, in the presence of noise. We now present the results of a few numerical simulations of Eqs. (13) with reaction terms and diffusion coefficients similar to some of the models mentioned above. More precisely, we use reaction terms of the form

$$R_N(N,W,S)=NS, \quad R_S(N,W,S)=-NS,$$

$$R_W(N,W,S)=0,$$

and a stochastic nonlinear diffusion coefficient $D^N(N,W,S)=D_0^N(1+\sigma)NS$, where σ is a random number with a triangular distribution of support $[-\rho,\rho]$, $0<\rho\leqslant 1$, as in Ref. [61]. Randomness in D^N represents inhomogeneities in the agar [61]. Note that D^N vanishes when either N or S are zero. According to Ref. [61], this reflects the fact that bacteria move slowly when N or S are small. Variations of D^N with W are neglected in the simulations below. As a consequence, the equation for W decouples from the equations for N and S when $\boldsymbol{v}^{chem}=0$.

In order to avoid numerical instabilities, the reaction terms on the right-hand sides of Eqs. (13) are set to zero if N is less than some cutoff value (set to 0.005 in the numerics except for the simulations of Figs. 4 and 5, for which it is equal to 0.02). Finally, we replace $\boldsymbol{\nabla}S/S$ by $\boldsymbol{\nabla}S/(S+0.05)$ in the expression for $\boldsymbol{v}$ to numerically keep this quantity finite when S is small. Initial conditions are of the form $N=0.71\exp[-20(x^2+y^2)]$, $S=0.35$, and $W=W_0=\text{const}$, as was the case in Ref. [61].

In dry media, i.e., when W is small, a discussion similar to that of Sec. IV B but for arbitrary values of ξ_1 and ξ_2 indicates that gradients of W remain small. In other words, W is almost constant and Eqs. (13) are thus very similar to classical reaction-diffusion equations, such as those discussed in Ref. [61]. One therefore expects similar types of results, as

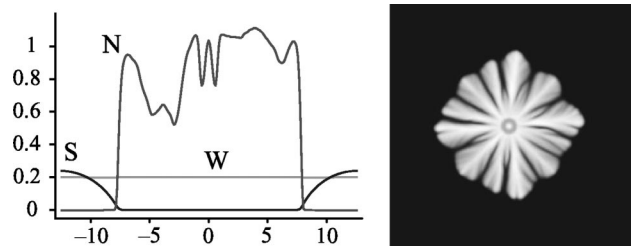

FIG. 4. Numerical solution of Eqs. (13) and (14) at $t=2700$. The parameters are $D^N=0.005(1+\sigma)NS$, where σ is a random number with a triangular distribution of support $[-1,1]$, $R_S=-NS$, $R_N=NS$, $R_W=0$, $k_0=1$, $\gamma=0$, $D^S=0.01$, and $D^W=0.005$. Left: profiles of N, S, and W as functions of position, along a horizontal line going through the middle of the colony. Right: gray-scale picture of N as a function of space.

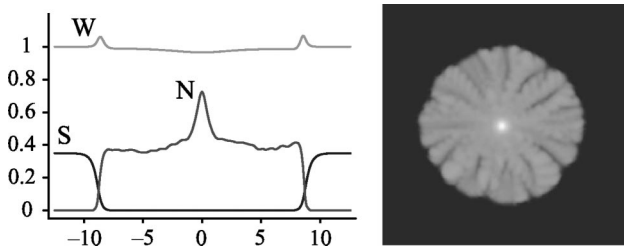

FIG. 6. Numerical solution of Eqs. (13) and (14) at $t=300$. The parameters are $D^N=0.05(1+\sigma)NS$, where σ is a random number with a triangular distribution of support $[-1,1]$, $R_S=-NS$, $R_N=NS$, $R_W=0$, $k_0=1$, $\gamma=0.0025$, $D^S=0.01$, and $D^W=0.005$. Left: profiles of N, S, and W as functions of position, along a horizontal line going through the middle of the colony. Right: gray-scale picture of N as a function of space.

exemplified in Figs. 4 and 5, for which $W_0=0.2$. In Fig. 4, $\gamma=0$, i.e., $\boldsymbol{v}^{chem}=0$. In Fig. 5, $\gamma=0.0025$ but the diffusion coefficient of S is smaller and the diffusion coefficient of W is larger than for the simulation of Fig. 4. All parameter values are given in the figure captions. When W is large, water is strongly influenced by the dynamics of N and S. Figures 6 and 7 show the results of two simulations of Eqs. (13) and (14) with $W_0=1$, for different values of γ and different values of the diffusion coefficient of S. The colony shown in Fig. 7 is the same as that shown in Fig. 3, but at a later time.

It is obvious from these simulations that very different colony shapes can be obtained from the advection-reaction-diffusion model (13),(14). In both Figs. 5 and 6, N has a peak in the center of the colony. This is due to the fact that in these simulations, the ratio D^N/D^S is relatively large (i.e., of order 1 or larger): nutrients diffuse slowly and, in regions where N is initially large, S is depleted before N can grow further.

B. Full hydrodynamic model

We now turn to the full hydrodynamic model. We first consider the chemotacticlike limit of Eqs. (12) and then illustrate the role of the small-scale forcing $\boldsymbol{F}_g$ produced by collective bacterial motions. These simulations all assume that the fluid is Newtonian. We also set $\lambda=\mu/3$, i.e., we neglect the bulk viscosity of the bacterial fluid. We first consider the chemotacticlike limit and compare the velocity $\boldsymbol{v}$ obtained from Eq. (11) to the velocity $\boldsymbol{v}^{chem}$ defined in Sec. IV. Initial conditions for N, S, and W are the same as for the simulations of the advection-reaction-diffusion model. The cutoff on the reaction terms is set to 0.002 in simulations of Sec. V B 1 and to 0.015 in Sec. V B 2.

1. Chemotacticlike limit

We can use the full hydrodynamic model to test the chemotactic limit discussed in Sec. IV. We cannot set to zero the diffusion coefficients in the equations for $\boldsymbol{v}^C$ and S, since this would lead to numerical instabilities. Moreover, decreasing these diffusion coefficients leads to an increase in the gradients of N and S so that the corresponding diffusive terms are never negligible. We thus expect the chemotactic limit to be singular.

In the absence of forcing in Eq. (11), the velocity field $\boldsymbol{v}$ remains close to $\boldsymbol{v}^C$ as long as the latter is not too large (i.e., as long as the nonlinear or viscous terms do not drive the equation for $\boldsymbol{v}^H$). As discussed in Sec. IV, if the reaction terms always dominate the dynamics of S, and if the time derivative of N/ρ is small, one expects

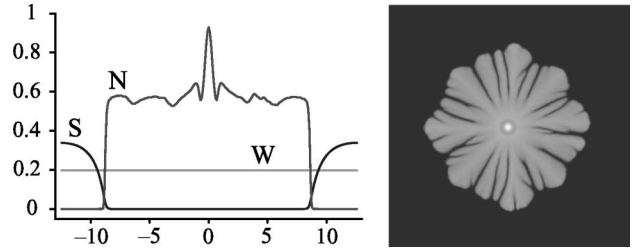

FIG. 5. Numerical solution of Eqs. (13) and (14) at $t=1700$. The parameters are $D^N=0.005(1+\sigma)NS$, where σ is a random number with a triangular distribution of support $[-1,1]$, $R_S=-NS$, $R_N=NS$, $R_W=0$, $k_0=1$, $\gamma=0.000\,25$, $D^S=0.005$, and $D^W=0.1$. Left: profiles of N, S, and W as functions of position, along a horizontal line going through the middle of the colony. Right: gray-scale picture of N as a function of space.

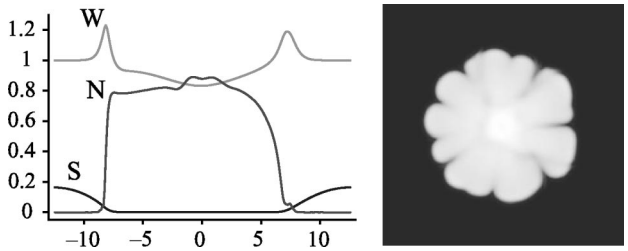

FIG. 7. Numerical solution of Eqs. (13) and (14) at $t=400$. The parameters are $D^N=0.05(1+\sigma)NS$, where σ is a random number with a triangular distribution of support $[-1,1]$, $R_S=-NS$, $R_N=NS$, $R_W=0$, $k_0=1$, $\gamma=0.01$, $D^S=0.1$, and $D^W=0.005$. Left: profiles of N, S, and W as functions of position, along a horizontal line going through the middle of the colony. Right: gray-scale picture of N as a function of space.

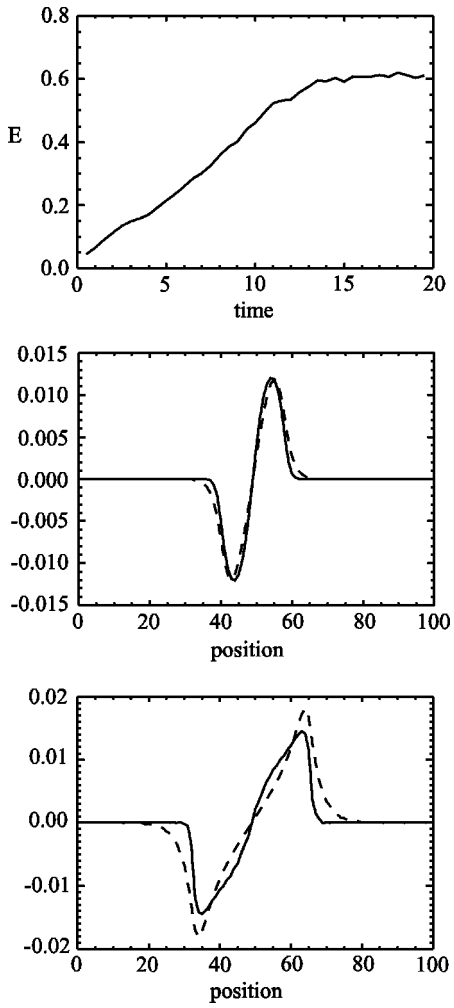

FIG. 8. Numerical solution of Eqs. (12), in the absence of forcing. The parameters are $D^N=0.005(1+\sigma)NS$, where σ is a random number with a triangular distribution of support $[-1,1]$, $R_S=-NS$, $R_N=NS$, $R_W=0$, $k_0=1$, $D^S=0.005$, $D^W=0.1$, $\mu=0.0002$, $W_0=0.02$, and $\gamma=1/900$. Top: error $E=\max(\|\boldsymbol{v}-\boldsymbol{v}^{chem}\|)/\max(\|\boldsymbol{v}\|)$ as a function of time. Middle: profiles of the x components of $\boldsymbol{v}^{chem}$ (solid line) and $\boldsymbol{v}$ (dashed line) at $t=5$. Bottom: same as above but for $t=20$. Position is measured in grid points (512 grid points correspond to a length of 8π).

$$\boldsymbol{v}\simeq\frac{2\gamma}{k_0}\frac{N}{\rho}\frac{\boldsymbol{\nabla}S}{f(S)}=\boldsymbol{v}^{chem}.$$

Numerical simulations of the full model (in the case of a Newtonian fluid) show that the relative difference $E=\max(\|\boldsymbol{v}-\boldsymbol{v}^{chem}\|)/\max(\|\boldsymbol{v}\|)$ remains of the order of a few percent only for a short period of time. Qualitative agreement however is fairly good, even at longer times. Figure 8 shows the results of a numerical simulation of Eqs. (12). The parameters are chosen such that μ (and $\lambda=\mu/3$) are small: this keeps $\boldsymbol{v}$ close to $\boldsymbol{v}^C$, as discussed above; W is small, so that $(\partial/\partial t)(N/\rho)=-(\partial/\partial t)(W/\rho)\ll 1$; D^S is small enough, *but not too small*, in order to have $R_S=NS>D^S\nabla^2 S$, at least in the beginning of the simulation; $F=0$. The error E, plotted as a function of time in the top panel of Fig. 8, increases rather rapidly and saturates to a value of about 60% at $t\simeq 15$. The middle panel of Fig. 8 shows cross sections of the x components of the two velocity fields $\boldsymbol{v}$ and $\boldsymbol{v}^{chem}$ at $t=5$, when E is less than 20%. The agreement between the two profiles is quite good. At $t=20$ (bottom panel of Fig. 8), when $E\simeq 60\%$, the agreement between the two profiles is only qualitative. At later times, the diffusion terms have become too large for the chemotactic limit to be significant. To summarize, in the absence of forcing in the hydrodynamic equation, the advection-reaction-diffusion model (13),(14) is expected to and does only give a qualitative description of the colony dynamics.

2. Small-scale forcing

In the presence of a small-scale forcing $\boldsymbol{F}_g\neq\boldsymbol{0}$, fine-scale structures develop within the colony and on its boundary, as shown in Fig. 9, which is a gray-scale rendering of the bacterial density N as a function of space for a Reynolds number $\mathrm{Re}\simeq 0.15$. In this simulation, $\eta=0$, $\boldsymbol{F}_e=\boldsymbol{0}$, and $\boldsymbol{F}_g$ is of the form $\boldsymbol{F}_g=N\rho\boldsymbol{f}$, where $\boldsymbol{f}$ is a white noise in time whose Fourier spectrum has Gaussian-distributed random phases and is supported on an annulus of width 5 and radius 11.25. The field $\boldsymbol{f}$ is also such that $\boldsymbol{\nabla}\cdot\boldsymbol{f}=0$. The small-scale forcing therefore vanishes outside the colony and increases with the amount of water present in the system (since it is assumed that bacteria are more active in wetter regions of the colony). We also show in Fig. 9 an enlargement of the middle-right part of the colony, with the velocity field $\boldsymbol{v}$ superimposed. Vortices and jets are visible within the colony. Their lifetime is longer than the time scale of the forcing (that is they persist over many time steps). A typical vortex size is about twice that of the small-scale forcing; the length of the jets is up to three times the diameter of a vortex. The dynamics is dominated by hydrodynamic motions: the chemotactic part of the velocity field ($\|\boldsymbol{v}^C\|$) is eight times as small as the hydrodynamic part ($\|\boldsymbol{v}^H\|$). The solenoidal part of $\boldsymbol{v}^C$ is about a thousand times as small as its compressible part. This is due to the fact that W varies slowly throughout the colony. Equation (10) indeed shows that when γ is constant, the curl of $\boldsymbol{v}^C$ can only grow through a term proportional to $\boldsymbol{\nabla}W\times\boldsymbol{\nabla}N$. Because vortices and jets are larger than the size of the imposed forcing, we believe that the mechanism at play here is that of transfer of energy from small to larger scales. However, no complete inverse cascade is clearly observed. Our results are nevertheless very promising, given that numerical constraints prevent us from imposing a realistic separation of scales between the forcing and the size of the colony.

The small-scale forcing affects the speed at which the colony boundary moves. Our numerical simulations indeed show that colonies grow faster when the Reynolds number is increased. Moreover, the vortices and jets located near the colony boundary act like a random noise that destabilizes the interface. We checked that very similar colony patterns are obtained even in the absence of noise in the bacterial diffusion coefficient.

VI. CONCLUSIONS

We have proposed a hydrodynamic model that gives a general description of bacterial colonies growing on soft agar

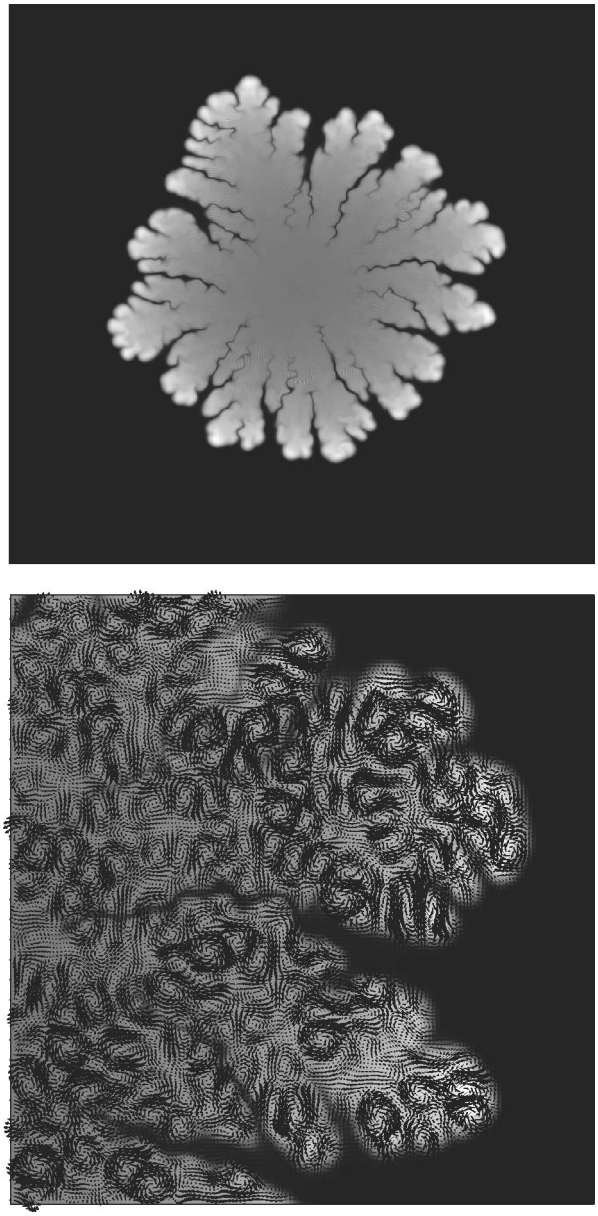

FIG. 9. Numerical simulation of Eqs. (12), in the presence of forcing. The parameters are $D^N=0.005(1+\sigma)NS$, where σ is a random number with a triangular distribution of support $[-1,1]$, $R_S=-NS$, $R_N=NS$, $R_W=0$, $k_0=1$, $D^S=0.005$, $D^W=0.1$, $\mu=0.01$, $W_0=1$, and $\gamma=0.000\,044$. Top: gray-scale picture of N as a function of space at $t=2000$. Bottom: velocity field $\boldsymbol{v}$ in the middle-right part of the colony. The length of each arrow is proportional to the amplitude of $\boldsymbol{v}$. The maximum of $||\boldsymbol{v}||$ is 0.01.

plates. In particular, a single set of equations captures motion *inside* as well as *at the boundary* of the colony. When bacterial collisions dominate, these equations formally reduce to a set of advection-reaction-diffusion equations. This approach thus provides a framework in which macroscopic reaction-diffusion models of bacterial colonies are justified on the basis of hydrodynamic considerations. The advection-reaction-diffusion equations we obtain treat the amount of water in the colony as one of their dependent variables. This allows us to describe colonies that are drier in the interior than at the boundary, in agreement with experimental observations. Finally, numerical simulations of the full hydrodynamic equations illustrate that our model is able to reproduce interesting colony shapes together with nontrivial dynamics inside the colony. In particular, collective behaviors such as whirls and jets can be generated by a small-scale random forcing. The basic principle behind the existence of these coherent structures is the transfer of energy from small to large scales in the equation describing the dynamics of the two-dimensional velocity field of the complex fluid. This phenomenon is analogous to the inverse cascade observed in two-dimensional turbulence. This description implies that vortices and jets are characteristic of bacterial systems confined to quasi-two-dimensional domains, as is the case in the experiments of Refs. [26,27]. It is different from the spontaneous organization observed in the model of self-propelled particles proposed by Vicsek *et al.* [36], where collective behaviors occur regardless of the dimension of the system.

We believe that this paper represents a first step towards the understanding of complex dynamics in bacterial colonies. The main characteristic of our model is that conservation equations for the bacterial, nutrient, and water concentrations are coupled to a single hydrodynamic equation for the velocity field of a complex fluid which consists of bacteria and water. Equations (12) are completely general and different types of bacteria will lead to different expressions for the reaction terms, the stress tensors, and the diffusion coefficients. Future work will deal with an experimental investigation of the rheologic and hydrodynamic properties of the bacterial fluid used in Ref. [26], an analysis of the reaction-diffusion model (13), and a detailed investigation of the coupling between colony shape and hydrodynamics, as described by Eqs. (12).

ACKNOWLEDGMENTS

We thank Neil Mendelson and Bachira Salhi for fruitful discussions and for sharing insights on their experimental work with us. We are also grateful to Greg Forest and Michael Rubinstein for interesting comments and suggestions about our model. This material is based upon work supported by the National Science Foundation under Grant Nos. 9909866 and 0075827 to J.L. and by CNRS (Centre National de la Recherche Scientifique)/NSF Grant No. 9166 to T.P.

APPENDIX A: HORIZONTAL VELOCITY PROFILE

In this appendix, we solve Brinkman's equation (1),

$$\mathbf{0}=-\boldsymbol{\nabla} p+\mu^*\nabla^2\boldsymbol{v}^W-\frac{\mu}{k}\boldsymbol{v}^W,$$

for a velocity field of the form $\boldsymbol{v}^W=f(z)\hat{\boldsymbol{x}}$, where z is the vertical coordinate pointing upward and $\hat{\boldsymbol{x}}$ is a unit vector in the horizontal direction x. We assume stress-free boundary conditions $df/dz=0$ at $z=0$ and no-slip boundary conditions $f(z)=0$ at $z=-H$. Moreover, in order to mimic a situation where fluid motion is triggered by bacteria swim-

ming near the top of the agar plate, we suppose that the pressure gradient $-\boldsymbol{\nabla} p$ is constant in a region of thickness h near the surface. These hypotheses only provide a cartoon of the real system, but they are sufficient to give an estimate of the vertical variation of the horizontal velocity field. For z between $-h$ and 0, the solution of

$$\mathbf{0}=-\frac{1}{\mu^*}\boldsymbol{\nabla} p+\frac{d^2 f}{dz^2}\hat{\boldsymbol{x}}-\alpha^2 f\hat{\boldsymbol{x}},\quad \alpha^2=\frac{\mu}{k\mu^*}$$

with $\boldsymbol{\nabla} p/\mu^*=C\hat{\boldsymbol{x}}$ and $df/dz=0$ at $z=0$ is

$$f(z)=-\frac{C}{\alpha^2}+C_1\cosh(\alpha z),$$

where the constant C_1 is to be determined. Similarly, for z between $-H$ and $-h$, the solution of

$$0=\frac{d^2 f}{dz^2}-\alpha^2 f,$$

with $f(-H)=0$ is

$$f(z)=\frac{C_2\sinh[\alpha(z+H)]}{\cosh(\alpha H)},$$

where C_2 is a yet-to-be-determined constant. The two constants C_1 and C_2 may be obtained by imposing the continuity of the global solution f and of its derivative at $z=-h$. We then have

$$f(z)=\begin{cases}-\dfrac{C}{\alpha^2}\left(1-\dfrac{\cosh(\alpha z)\cosh[\alpha(h-H)]}{\cosh(\alpha H)}\right) & \text{if } -h\leqslant z\leqslant 0\\[2ex] -\dfrac{C\sinh(\alpha h)\sinh[\alpha(z+H)]}{\alpha^2\cosh(\alpha H)} & \text{if } -H\leqslant z\leqslant -h.\end{cases}\tag{A1}$$

Figure 10 shows a plot of this function for $\alpha=1$, $H=10$, $h=1$, and $C=-1$. It illustrates the behavior of the velocity field in the region where the pressure gradient is nonvanishing, as well as the exponential decay of the velocity field outside of the layer of thickness h.

We can use the solution (A1) to calculate the coefficient $\zeta=\langle f^2\rangle/\langle f\rangle^2$, which appears in Eqs. (8), where $\langle\cdot\rangle$ indicates averaging over $[-h,0]$. The formula is a little complicated, but simplifies in the limit as $\alpha H\to\infty$. Since the actual value of H is irrelevant as long as it is much larger than h, taking this limit is legitimate. We then get

$$\zeta=\frac{\alpha h}{2}\,\frac{-1+4(2+\alpha h)\exp(2\alpha h)+(8\alpha h-7)\exp(4\alpha h)}{1+2(2\alpha h-1)\exp(2\alpha h)+(2\alpha h-1)^2\exp(4\alpha h)}.$$

A plot of this coefficient as a function of αh (not shown) reveals that ζ is always between 1 and 1.022, with a maximum reached for $\alpha h\simeq 2.9$. Therefore, one can take $\zeta\simeq 1$ as long as vertical averaging is performed over a layer of depth h, that is, over the region where bacteria are active.

APPENDIX B: TWO-PHASE FLUID APPROACH TO THE HYDRODYNAMIC EQUATIONS

In this appendix, we discuss how the hydrodynamic equations for the mixture of bacteria and water may be obtained from a two-phase fluid approach.

1. General setup

We start by assuming that bacteria and water can be considered as two interpenetrating interacting continua [38,62,63] and then discuss under which conditions one can simplify the resulting model. The two-fluid description assumes that it is legitimate to talk of ''bacterial fluid particles,'' which in turn supposes that one can envision, at least conceptually, a fluid made of bacteria. We first write the continuity and momentum equations for each of the fluids, an approach similar to that developed in Ref. [64] for multicomponent reacting systems. Recall that we denote by W the mass of water and by N the mass of bacteria per unit volume. Let $\boldsymbol{v}^W$ and $\boldsymbol{v}^N$ be the velocity fields for the water and the bacteria, respectively. The continuity equations for W and N read

$$\frac{\partial W}{\partial t}+\boldsymbol{\nabla}\cdot(W\boldsymbol{v}^W)=R_W+\boldsymbol{\nabla}\cdot(D^W\boldsymbol{\nabla} W),\tag{B1}$$

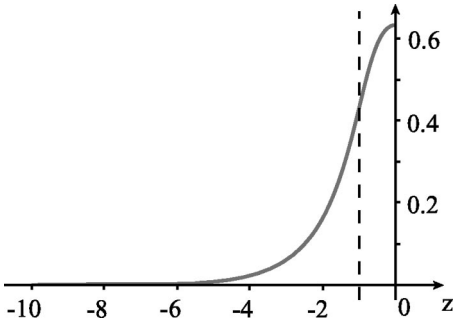

FIG. 10. Plot of the solution given by Eq. (A1) with $\alpha=1$, $H=10$, $h=1$, and $C=-1$. The dashed line is the line of equation $z=-h$, which separates the region near the surface ($z=0$) where the pressure gradient is finite from the region where no pressure gradient is imposed.

$$\frac{\partial N}{\partial t}+\nabla\cdot(N\boldsymbol{v}^N)=R_N, \tag{B2}$$

where R_N and R_W are defined in the main part of the text and $\nabla\cdot(D^W\nabla W)$ in the equation for the concentration of water describes dispersion [45] in the porous medium. To get an intuitive understanding of what dispersion does, assume that the bottom of the agar plate is wetter than its top. We then expect water to move upward by capillarity. At a macroscopic level, water will appear to ''diffuse'' towards the top of the plate. Similarly, horizontal variations in the concentration of water in the agar will lead to water displacement across the plate. The dispersion coefficient D^W is proportional to the gradient with respect to W of the capillary pressure and is, in general, a power law function of W [65]. It should not be confused with the molecular diffusivity, normalized by the porosity of the medium, which typically affects the concentration field of a fluid miscible in a given solvent. The inclusion of dispersion in the continuity equation for W may be justified as follows. In the absence of bacteria and if the presence of air in the porous medium is taken into account, one may assume that the velocity fields of air and water inside the agar follow Darcy's equation for a two-phase fluid [45]. The water velocity field can then be expressed in terms of the velocity field of the air-water mixture and of the capillary pressure. When substituted into the continuity equation for water, this leads to an advection term [of the form $\nabla\cdot(W\boldsymbol{v}^W)$ as above, but where $\boldsymbol{v}^W$ now stands for the velocity field of the air-water mixture] corrected by a dispersion term [as on the right-hand side of Eq. (B1)], proportional to the gradient of the capillary pressure [45]. When bacteria are present, Darcy's equation no longer describes the dynamics of $\boldsymbol{v}^W$, since viscous as well as inertial effects have to be taken into account. In order to keep our model as simple as possible, we include dispersion in the continuity equation for W instead of adding capillary pressure terms to the equation for $\boldsymbol{v}^W$ (or instead of introducing a third velocity field for the air in the porous medium). Given the large aspect ratio of the plate, the water concentration W will be considered homogeneous in the vertical direction.

If we now define $\rho=N+W$, we obtain the following equation from Eqs. (B1) and (B2):

$$\frac{\partial\rho}{\partial t}+\nabla\cdot(W\boldsymbol{v}^W+N\boldsymbol{v}^N)=R_N+R_W+\nabla\cdot(D^W\nabla W).$$

This equation can then be written as a continuity equation for ρ:

$$\frac{\partial\rho}{\partial t}+\nabla\cdot(\rho\boldsymbol{v})=R_N+R_W+\nabla\cdot(D^W\nabla W), \tag{B3}$$

where the velocity field $\boldsymbol{v}$ is defined by

$$\boldsymbol{v}=\frac{W\boldsymbol{v}^W+N\boldsymbol{v}^N}{W+N}=\frac{1}{\rho}(W\boldsymbol{v}^W+N\boldsymbol{v}^N). \tag{B4}$$

The quantity ρ is the density of the mixture or two-phase fluid [38,63] made of bacteria and water. If this mixture can be considered as a single fluid, then its velocity field is given by $\boldsymbol{v}$, which is the mass-weighted average of the water and bacterial velocity fields.

The equations for the conservation of linear momentum[3] for water and bacteria read

$$W\frac{\partial}{\partial t}\boldsymbol{v}^W+W(\boldsymbol{v}^W\cdot\nabla)\boldsymbol{v}^W=\nabla\cdot\boldsymbol{T}^W+\boldsymbol{F}^W, \tag{B5}$$

$$N\frac{\partial}{\partial t}\boldsymbol{v}^N+N(\boldsymbol{v}^N\cdot\nabla)\boldsymbol{v}^N=\nabla\cdot\boldsymbol{T}^N+\boldsymbol{F}^N, \tag{B6}$$

where $\boldsymbol{T}^W$ and $\boldsymbol{T}^N$ are the stress tensors for water and bacteria, respectively, and the external forces per unit volume $\boldsymbol{F}^W$ and $\boldsymbol{F}^N$ can be written as

$$\boldsymbol{F}^W=\boldsymbol{F}_i^W+\boldsymbol{F}_s^W+\boldsymbol{F}_e^W,$$

$$\boldsymbol{F}^N=\boldsymbol{F}_i^N+\boldsymbol{F}_s^N+\boldsymbol{F}_g^N.$$

Here, $\boldsymbol{F}_i^W=-\boldsymbol{F}_i^N$ describes internal interactions between bacteria and water, $\boldsymbol{F}_s^W$ and $\boldsymbol{F}_s^N$ describe interactions with the substrate [according to Brinkman's theory, these forces are damping forces, as in Eq. (1)], $\boldsymbol{F}_e^W$ and $\boldsymbol{F}_g^N$ correspond to changes in linear momentum due to external forces (such as gravity) and to bacterial activity, respectively. The force $\boldsymbol{F}_g^N$

[3]These equations express Newton's law for a given ensemble of ''particles'' which move along with the fluid (that is, $Wd\tau$ and $Nd\tau$, where $d\tau$ is a volume element, are kept constant) [66]. As a consequence, mass fluxes do not give rise to force terms on the right-hand side of the momentum equations [63]. Such equations could also be obtained by writing that linear momentum is conserved for a volume of fluid moving along with the flow. The corresponding balance equation would then contain terms describing a change in momentum due to mass increase or due to mass fluxes. These terms would then cancel out when the balance equation is combined with the corresponding continuity equation to give an equation like (B5) or (B6).

describes subgrid scale dynamics in the bacterial fluid and is thus different from $\boldsymbol{F}_i^N = -\boldsymbol{F}_i^W$. Each of the momentum equations may be rewritten as an equation for the local conservation of linear momentum. For instance, by combining Eqs. (B2) and (B6), one obtains

$$\frac{\partial}{\partial t}(N\boldsymbol{v}^N) + \boldsymbol{\nabla}\cdot(N\boldsymbol{v}^N\boldsymbol{v}^N) = \boldsymbol{\nabla}\cdot\boldsymbol{T}^N + R_N\boldsymbol{v}^N + \boldsymbol{F}_i^N + \boldsymbol{F}_s^N + \boldsymbol{F}_g^N, \tag{B7}$$

where $\boldsymbol{\nabla}\cdot(N\boldsymbol{v}^N\boldsymbol{v}^N)$ is a vector whose jth component in Cartesian coordinates is $\boldsymbol{\nabla}\cdot(N\boldsymbol{v}^N v_j^N)$ and v_j^N is the jth component of $\boldsymbol{v}^N$. The fact that bacteria are living organisms gives rise to changes in linear momentum first because the mass of a fluid particle changes as it is advected by the fluid (term in $R_N\boldsymbol{v}^N$) and second because bacterial activity may, at the hydrodynamic scale, appear as a small-scale forcing, which is accounted for by $\boldsymbol{F}_g^N$.

Similarly, by combining Eqs. (B1) and (B5), one gets an equation for the local conservation of linear momentum of water, which reads

$$\frac{\partial}{\partial t}(W\boldsymbol{v}^W) + \boldsymbol{\nabla}\cdot(W\boldsymbol{v}^W\boldsymbol{v}^W) = \boldsymbol{\nabla}\cdot\boldsymbol{T}^W + R_W\boldsymbol{v}^W + \boldsymbol{F}^W + \boldsymbol{v}^W\boldsymbol{\nabla}\cdot(D^W\boldsymbol{\nabla}W). \tag{B8}$$

By adding Eqs. (B7) and (B8), we get

$$\frac{\partial}{\partial t}(\rho\boldsymbol{v}) + \boldsymbol{\nabla}\cdot(\rho\boldsymbol{v}\boldsymbol{v}) = \boldsymbol{\nabla}\cdot\boldsymbol{T} + \tilde{\boldsymbol{F}}, \tag{B9}$$

where

$$\boldsymbol{T} = \boldsymbol{T}^W + \boldsymbol{T}^N - N\boldsymbol{v}^N(\boldsymbol{v}^N - \boldsymbol{v}) - W\boldsymbol{v}^W(\boldsymbol{v}^W - \boldsymbol{v})$$

and

$$\begin{aligned}\tilde{\boldsymbol{F}} &= \boldsymbol{F}^W + \boldsymbol{F}^N + R_N\boldsymbol{v}^N + R_W\boldsymbol{v}^W + \boldsymbol{v}^W\boldsymbol{\nabla}\cdot(D^W\boldsymbol{\nabla}W)\\ &= \boldsymbol{F}_s^W + \boldsymbol{F}_s^N + \boldsymbol{F}_e^W + \boldsymbol{F}_g^N + R_N\boldsymbol{v}^N + R_W\boldsymbol{v}^W + \boldsymbol{v}^W\boldsymbol{\nabla}\cdot(D^W\boldsymbol{\nabla}W)\\ &= \boldsymbol{F}_s + \tilde{\boldsymbol{F}}_e + \tilde{\boldsymbol{F}}_g.\end{aligned}$$

Here, $\boldsymbol{F}_s = \boldsymbol{F}_s^W + \boldsymbol{F}_s^N$ describes interaction of the fluid with the substrate, $\tilde{\boldsymbol{F}}_e = \boldsymbol{F}_e^W + R_W\boldsymbol{v}^W + \boldsymbol{v}^W\boldsymbol{\nabla}\cdot(D^W\boldsymbol{\nabla}W)$ corresponds to changes in linear momentum due to external forces and transfer of water between the agar plate, the colony, and the surrounding air, and $\tilde{\boldsymbol{F}}_g = \boldsymbol{F}_g^N + R_N\boldsymbol{v}^N$ accounts for changes in linear momentum due to bacterial growth and bacterial activity. The tensor $\boldsymbol{T}$ is the sum of the stress tensors $\boldsymbol{T}^N$ and $\boldsymbol{T}^W$ of bacteria and water, corrected by terms involving each velocity field $\boldsymbol{v}^N$ and $\boldsymbol{v}^W$, as well as their mass-weighted average $\boldsymbol{v}$.

A closed set of equations for our system consists, for instance, of the continuity equations (2) and (B3), of the momentum equation (B9), and of the continuity and momentum equations for water (B1) and (B5), together with appropriate boundary conditions and expressions for the stress tensors $\boldsymbol{T}^W$ and $\boldsymbol{T}^N$. The difficulty with such a description is that it requires some knowledge of the internal force $\boldsymbol{F}_i^W = -\boldsymbol{F}_i^N$, which describes interactions between bacteria and water. Our next step is therefore to reduce this system to coupled equations which only involve $\boldsymbol{v}$, rather than $\boldsymbol{v}^N$ and $\boldsymbol{v}^W$. More precisely, given the relatively high bacterial density in the system, and given the fact that no motion is observed in the absence of bacteria or if bacteria are dead, it is legitimate to assume that most of the dynamics is due to the bacteria. At the hydrodynamic scale, bacteria and water move as a single fluid, so that one can expect $(\boldsymbol{v}^N - \boldsymbol{v}^W)^2$ to be small, say, $\boldsymbol{v}^W - \boldsymbol{v}^N = \epsilon\boldsymbol{m}$, where $||\boldsymbol{m}|| = O(||\boldsymbol{v}^N||)$ and $\epsilon \ll 1$. The mean velocity field $\boldsymbol{v}$ is given by $\boldsymbol{v} = \boldsymbol{v}^N + \epsilon\delta\boldsymbol{m}$ and the velocity terms in the expression for the tensor $\boldsymbol{T}$ read

$$N\boldsymbol{v}^N(\boldsymbol{v}^N - \boldsymbol{v}) + W\boldsymbol{v}^W(\boldsymbol{v}^W - \boldsymbol{v}) = \rho\,\delta(1-\delta)\epsilon^2\boldsymbol{m}\boldsymbol{m}.$$

They are therefore negligible when compared to $\rho(\boldsymbol{v}^N)^2 = O(\rho\boldsymbol{v}^2)$. When combined to the continuity equation (B3), the momentum equation (B9) becomes Eq. (5),

$$\rho\frac{\partial\boldsymbol{v}}{\partial t} + \rho(\boldsymbol{v}\cdot\boldsymbol{\nabla})\boldsymbol{v} = \boldsymbol{\nabla}\cdot\boldsymbol{T} + \boldsymbol{F},$$

where

$$\begin{aligned}\boldsymbol{F} &= \tilde{\boldsymbol{F}} - \boldsymbol{v}R_N - \boldsymbol{v}R_W - \boldsymbol{v}\boldsymbol{\nabla}\cdot(\boldsymbol{\nabla}D^W W)\\ &= \boldsymbol{F}_s + \boldsymbol{F}_e^W + \boldsymbol{F}_g^N + R_N(\boldsymbol{v}^N - \boldsymbol{v}) + R_W(\boldsymbol{v}^W - \boldsymbol{v})\\ &\quad + (\boldsymbol{v}^W - \boldsymbol{v})\boldsymbol{\nabla}\cdot(D^W\boldsymbol{\nabla}W)\\ &= \boldsymbol{F}_s + \boldsymbol{F}_e + \boldsymbol{F}_g\end{aligned}$$

and $\boldsymbol{F}_e = \boldsymbol{F}_e^W + R_W(\boldsymbol{v}^W - \boldsymbol{v}) + (\boldsymbol{v}^W - \boldsymbol{v})\boldsymbol{\nabla}\cdot(D^W\boldsymbol{\nabla}W)$, $\boldsymbol{F}_g = \boldsymbol{F}_g^N + R_N(\boldsymbol{v}^N - \boldsymbol{v})$. With the assumptions discussed above, we can replace $\boldsymbol{\nabla}\cdot\boldsymbol{T}$ by $\boldsymbol{\nabla}\cdot(\boldsymbol{T}^W + \boldsymbol{T}^N)$, and neglect the last terms in the expressions for $\boldsymbol{F}_e$ and $\boldsymbol{F}_g$. The force $\boldsymbol{F}_s = \boldsymbol{F}_s^W + \boldsymbol{F}_s^N$ is typically of the form $\boldsymbol{F}_s = -\alpha^W\boldsymbol{v}^W - \alpha^N\boldsymbol{v}^N$, where $\alpha^{N,W}$ are friction coefficients that depend on the elastic properties of the two fluids and on the geometry of the porous medium [43]. This force can then be rewritten as

$$\boldsymbol{F}_s = -\alpha^W(\boldsymbol{v}^N + \epsilon\boldsymbol{m}) - \alpha^N\boldsymbol{v}^N = -(\alpha^W + \alpha^N)\boldsymbol{v} + O(\epsilon\boldsymbol{m})$$

and can therefore be approximated by $\boldsymbol{F}_s \simeq -\alpha\boldsymbol{v}$, where α describes the interaction of the fluid with the porous medium. If we take δ as a parameter, Eqs. (2), (B3), and (5), with $W = \delta\rho$, $N = (1-\delta)\rho$, and appropriate boundary conditions and expressions for $\boldsymbol{T}^N$ and $\boldsymbol{T}^W$, form a closed system for the velocity field $\boldsymbol{v}$, the density ρ, and the nutrient concentration field S. They are the hydrodynamic equations for a single bacterial fluid that consists of densely packed bacteria and water. We expect them to be valid within the colony, i.e., away from its boundary.

Near the boundary of the colony, δ experiences large variations and, therefore, cannot be treated as a parameter.

An equation for this quantity should thus be included in the model. It turns out that it is easier to use N and W as dependent variables. The continuity equation (B2) can then be rewritten as a reaction-diffusion equation for N,

$$\frac{\partial N}{\partial t}+\boldsymbol{\nabla}\cdot(N\boldsymbol{v})=R_N+\boldsymbol{\nabla}\cdot[N(\boldsymbol{v}-\boldsymbol{v}^N)]=R_N-\boldsymbol{\nabla}\cdot\boldsymbol{j}^N,$$

where $\boldsymbol{j}^N=N(\boldsymbol{v}^N-\boldsymbol{v})=-\epsilon N\delta\boldsymbol{m}$ is the flux of bacteria through a line advected at the mean velocity $\boldsymbol{v}$. With $\boldsymbol{j}^N=-D^N\boldsymbol{\nabla}N$, we obtain Eq. (3). Note that since $\boldsymbol{j}^N=N(\boldsymbol{v}^N-\boldsymbol{v})=WN(\boldsymbol{v}^N-\boldsymbol{v}^W)/\rho$, it is reasonable to assume that $||D^N||$ is proportional to N and W. Also note that higher-order terms may be included in Eqs. (7), provided a ''closure relation'' for $\boldsymbol{v}^W-\boldsymbol{v}^N$ is added to the model.

2. Case of a Newtonian fluid

The stress tensors $\boldsymbol{T}^W$ and $\boldsymbol{T}^N$ are written as

$$\boldsymbol{T}^W=-p^WI+\boldsymbol{\tau}^W,\quad \boldsymbol{T}^N=-p^NI+\tau^N,$$

where the isotropic parts p^W and p^N are the water and bacterial pressures, and $\boldsymbol{\tau}^W$ and $\boldsymbol{\tau}^N$ are strain-related stresses. We now express the stress tensors $\boldsymbol{\tau}^W$ and $\boldsymbol{\tau}^N$ in terms of $\boldsymbol{v}$, N, and W, in the case where bacteria behave as a Newtonian fluid. We thus assume that

$$\boldsymbol{\nabla}\cdot\boldsymbol{\tau}^W=\mu^W\nabla^2\boldsymbol{v}^W$$

$$\boldsymbol{\nabla}\cdot\boldsymbol{\tau}^N=\mu^N\nabla^2\boldsymbol{v}^N+\lambda^N\boldsymbol{\nabla}(\boldsymbol{\nabla}\cdot\boldsymbol{v}^N),\qquad \text{(B10)}$$

where μ^W and μ^N are the water and bacterial viscosities, and λ^N is a second viscosity coefficient for the bacteria (which form a compressible fluid). Since $\boldsymbol{v}^N$ and $\boldsymbol{v}^W$ are comparable and if we consider that $\mu^W\simeq\mu^N$, we can simplify the viscous terms, which become

$$\begin{aligned}
&\mu^W\nabla^2\boldsymbol{v}^W+\mu^N\nabla^2\boldsymbol{v}^N+\lambda^N\boldsymbol{\nabla}(\boldsymbol{\nabla}\cdot\boldsymbol{v}^N)\\
&\quad=(\mu^W+\mu^N)\nabla^2\boldsymbol{v}+\nabla^2\left[\frac{N\mu^W-W\mu^N}{N+W}(\boldsymbol{v}^W-\boldsymbol{v}^N)\right]\\
&\quad+\lambda^N\boldsymbol{\nabla}\left[\boldsymbol{\nabla}\cdot\left(\boldsymbol{v}+\frac{W}{N+W}(\boldsymbol{v}^N-\boldsymbol{v}^W)\right)\right]\\
&\quad=(\mu^W+\mu^N)\nabla^2\boldsymbol{v}+\nabla^2[\{(1-\delta)\mu^W-\delta\mu^N\}\epsilon\boldsymbol{m}]\\
&\quad+\lambda^N\boldsymbol{\nabla}[\boldsymbol{\nabla}\cdot(\boldsymbol{v}-\delta\epsilon\boldsymbol{m})]\\
&\quad\simeq\mu\nabla^2\boldsymbol{v}+\lambda\boldsymbol{\nabla}(\boldsymbol{\nabla}\cdot\boldsymbol{v}),
\end{aligned}$$

where $\mu=\mu^W+\mu^N$ and $\lambda=\lambda^N$. Note that the expression for μ is different from the viscosity of a dilute suspension, for which μ is a function of the volume fraction of the particulate phase [29]. This is because in a two-phase fluid model, one does not distinguish between a solvent and a solute.

[1] *Bacteria as Multicellular Organisms*, edited by J.A. Shapiro and M. Dworkin (Oxford University Press, Oxford, New York, 1997).

[2] J.A. Shapiro, in *The Bacteria* (Academic Press, New York, 1986), Vol. X, Chap. 2.

[3] H. Fujikawa and M. Matsushita, J. Phys. Soc. Jpn. **58**, 3875 (1989).

[4] T. Matsuyama and M. Matsushita, Crit. Rev. Microbiol. **19**, 117 (1993).

[5] I. Cohen, A. Czirók, and E. Ben-Jacob, Physica A **233**, 678 (1996).

[6] I. Golding, Y. Kozlovsky, I. Cohen, and E. Ben-Jacob, Physica A **260**, 510 (1998).

[7] H. Fujikawa and M. Matsushita, J. Phys. Soc. Jpn. **60**, 88 (1991).

[8] M. Ohgiwari, M. Matsushita, and T. Matsuyama, J. Phys. Soc. Jpn. **61**, 816 (1992).

[9] N.H. Mendelson and B. Salhi, J. Bacteriol. **178**, 1980 (1996).

[10] Y. Kozlovsky, I. Cohen, I. Golding, and E. Ben-Jacob, Phys. Rev. E **59**, 7025 (1999).

[11] J.A. Shapiro, Sci. Prog. **76**, 399 (1994).

[12] E.O. Budrene and H.C. Berg, Nature (London) **349**, 630 (1991).

[13] E.O. Budrene and H.C. Berg, Nature (London) **376**, 49 (1995).

[14] Y. Blat and M. Eisenbach, J. Bacteriol. **177**, 1683 (1995).

[15] J.A. Shapiro, BioEssays **17**, 597 (1995).

[16] E.F. Keller and L.A. Segel, J. Theor. Biol. **30**, 225 (1971).

[17] E.F. Keller and L.A. Segel, J. Theor. Biol. **30**, 235 (1971).

[18] M.A. Rivero, R.T. Tranquillo, H.M. Buettner, and D.A. Lauffenburger, Chem. Eng. Sci. **44**, 2881 (1989).

[19] M. Mimura, H. Sakaguchi, and M. Matsushita, Physica A **282**, 283 (2000).

[20] E. Ben-Jacob, I. Cohen, O. Shochet, I. Aranson, H. Levine, and L. Tsimring, Nature (London) **373**, 566 (1995).

[21] L. Tsimring, H. Levine, I. Aranson, E. Ben-Jacob, I. Cohen, O. Shochet, and W.N. Reynolds, Phys. Rev. Lett. **75**, 1859 (1995).

[22] R. Tyson, L.G. Stern, and R.J. LeVeque, J. Math. Biol. **41**, 455 (2000).

[23] S.E. Esipov and J.A. Shapiro, J. Math. Biol. **36**, 249 (1998).

[24] E. Ben-Jacob, O. Schochet, A. Tenenbaum, I. Cohen, A. Czirók, and T. Vicsek, Nature (London) **368**, 46 (1994).

[25] E. Ben-Jacob, O. Shochet, A. Tenenbaum, and I. Cohen, Phys. Rev. E **53**, 1835 (1996).

[26] N.H. Mendelson, A. Bourque, K. Wilkening, K.R. Anderson, and J.C. Watkins, J. Bacteriol. **181**, 600 (1999).

[27] X.-L. Wu and A. Libchaber, Phys. Rev. Lett. **84**, 3017 (2000).

[28] J.O. Kessler, in *International Conference on Differential Equations*, edited by B. Fiedler, K. Gröger, and J. Sprekels (World Scientific, Singapore, 2000), Vol. 2, pp. 1284–1287.

[29] D.H. Everett, *Basic Principles of Colloid Science* (The Royal Society of Chemistry, London, 1988).

[30] E. Guyon, J.P. Hulin, L. Petit, and C. Mitescu, *Physical Hydrodynamics* (Oxford University Press, Oxford, New York, 2001).

[31] M.A. Bees, P. Andresén, E. Mosekilde, and M. Givskov, J. Math. Biol. **40**, 27 (2000).

[32] T.J. Pedley and J.O. Kessler, Annu. Rev. Fluid Mech. **24**, 313 (1992).
[33] A.M. Metcalfe and T.J. Pedley, J. Fluid Mech. **370**, 249 (1998).
[34] M. Ramia, D.L. Tullock, and N. Phan-Thien, Biophys. J. **65**, 755 (1993).
[35] J. Toner and Y. Tu, Phys. Rev. E **58**, 4828 (1998).
[36] T. Vicsek, A. Czirók, E. Ben-Jacob, I. Cohen, and O. Shochet, Phys. Rev. Lett. **75**, 1226 (1995).
[37] A. Czirók, H.E. Stanley, and T. Vicsek, J. Phys. A **30**, 1375 (1997).
[38] D.A. Drew, Annu. Rev. Fluid Mech. **15**, 261 (1983).
[39] U. Frisch, *Turbulence* (Cambridge University Press, Cambridge, 1995).
[40] C. Foias, O. Manley, R. Rosa, and R. Temam, *Navier-Stokes Equations and Turbulence*, Encyclopedia of Mathematics and its Applications Vol. 83 (Cambridge University Press, Cambridge, 2001).
[41] C.D. Amsler, M. Cho, and P. Matsumura, J. Bacteriol. **175**, 6238 (1993).
[42] R.M. Macnab, in *Escherichia coli and Salmonella: Cellular and Molecular Biology*, edited by F.C. Neidhardt, R. Curtiss III, J.L. Ingraham, E.C.C. Lin, K.B. Low, B. Magasanik, W.S. Reznikoff, M. Riley, M. Schaechter, and H.E. Umbarger (American Society for Microbiology, Washington, D. C., 1996), pp. 123–145.
[43] H.C. Brinkman, Appl. Sci. Res., Sect. A **1**, 27 (1947).
[44] D.F. James and A.M.J. Davis, J. Fluid Mech. **426**, 47 (2001).
[45] A.E. Scheidegger, *The Physics of Flow Through Porous Media* (MacMillan, New York, 1960), see Chap. 9.
[46] J.R. Philip, Annu. Rev. Fluid Mech. **2**, 177 (1970).
[47] T.L. Hill, *An Introduction to Statistical Thermodynamics* (Dover, New York, 1988), see p. 288.
[48] B.T. Kress and D. Montgomery, J. Plasma Phys. **64**, 371 (2000).
[49] J.D. Murray, *Mathematical Biology*, 2nd ed. (Springer-Verlag, Berlin, 1993).
[50] D.A. Brown and H.C. Berg, Proc. Natl. Acad. Sci. U.S.A. **71**, 1388 (1974).
[51] J.-J. Xu, *Interfacial Wave Theory of Pattern Formation: Selection of Dendritic Growth and Viscous Fingering in Hele-Shaw Flow, Springer Series in Synergetics* (Springer, Berlin, 1998).
[52] W. van Saarloos, Phys. Rep. **301**, 9 (1998).
[53] R.E. Goldstein, D.J. Muraki, and D.M. Petrich, Phys. Rev. E **53**, 3933 (1996).
[54] C.B. Muratov and V.V. Osipov, Phys. Rev. E **53**, 3101 (1996).
[55] C.B. Muratov, Phys. Rev. E **54**, 3369 (1996).
[56] A. De Wit and G.M. Homsy, J. Chem. Phys. **110**, 8663 (1999).
[57] J. Yang, A. D'Onofrio, S. Kalliadasis, and A. De Wit, J. Chem. Phys. **117**, 9395 (2002).
[58] D. Horváth, T. Bánsági, Jr., and A. Tóth, J. Chem. Phys. **117**, 4399 (2002).
[59] D.A. Kessler and H. Levine, Nature (London) **394**, 556 (1998).
[60] S. Kitsunezaki, J. Phys. Soc. Jpn. **66**, 1544 (1997).
[61] K. Kawasaki, A. Mochizuki, M. Matsushita, T. Umeda, and N. Shigesada, J. Theor. Biol. **188**, 177 (1997).
[62] M.F. Göz, J. Fluid Mech. **240**, 379 (1992).
[63] D. Gidaspow, *Multiphase Flow and Fluidization* (Academic Press, Boston, 1993).
[64] H.G. Othmer, J. Chem. Phys. **64**, 460 (1975).
[65] H.T. Davis, R.A. Novy, L.E. Scriven, and P.G. Toledo, J. Phys.: Condens. Matter **2**, SA457 (1990).
[66] D.J. Tritton, *Physical Fluid Dynamics* (Oxford University Press, Oxford, New York, 1988).